AMERICAN UNIVERSITY OF BEIRUT

ANTICANCER ACTIVITY AND UPTAKE MECHANISMS OF THYMOQUINONE-LOADED CUBOSOMAL NANOPARTICLES IN HUMAN BREAST CANCER

By
RANA IYAD SARIEDDINE

A dissertation
submitted in partial fulfilment of the requirements
for the degree of Master of Science
to the Department of Biology
of the Faculty of Arts and Sciences
at the American University of Beirut

Beirut, Lebanon
December 2019

AMERICAN UNIVERSITY OF BEIRUT

ANTICANCER ACTIVITY AND UPTAKE MECHANISMS OF THYMOQUINONE-LOADED CUBOSOMAL NANOPARTICLES IN HUMAN BREAST CANCER

By
RANA IYAD SARIEDDINE

Approved by:

Dr. Hala Gali-Muhtasib, Professor — Advisor
Department of Biology, and Department of Anatomy, Cell Biology, Physiological Sciences, American University of Beirut, Lebanon

Dr. Rabih Talhouk, Professor — Member of Committee
Department of Biology, American University of Beirut, Lebanon

Dr. Diana Jaalouk, Associate Professor — Member of Committee
Department of Biology, American University of Beirut, Lebanon

Dr. Mohammed Mehanna, Associate Professor — Member of Committee
Department of Pharmaceutical Technology, Beirut Arab University

Date of thesis defense: December 19th, 2019

AMERICAN UNIVERSITY OF BEIRUT

THESIS, DISSERTATION, PROJECT RELEASE FORM

Student Name:

Sarieddine	Rana	Iyad
Last	First	Middle

⊗ Master's Thesis ○ Master's Project ○ Doctoral Dissertation

☒ I authorize the American University of Beirut to: (a) reproduce hard or electronic copies of my thesis, dissertation, or project; (b) include such copies in the archives and digital repositories of the University; and (c) make freely available such copies to third parties for research or educational purposes.

☐ I authorize the American University of Beirut, to: (a) reproduce hard or electronic copies of it; (b) include such copies in the archives and digital repositories of the University; and (c) make freely available such copies to third parties for research or educational purposes
after: **One ---- year from the date of submission of my thesis, dissertation, or project.**

Two ---- years from the date of submission of my thesis, dissertation, or project.

Three ---- years from the date of submission of my thesis, dissertation, or project.

Rana Sarieddine 22/01/2020

Signature Date

ACKNOWLEDGMENTS

During my two-year stay at AUB, I have received a lot of support from a great number of people inside and outside of AUB.

First, I would like to thank my advisor, Dr. Hala Muhtasib, for she always brings positive energy to the laboratory no matter what the situation is. Being her student helped me become more independent and confident in my work.

Moreover, I would like to thank Dr. Diana Jaalouk for all the fruitful lessons given to us during her lectures. She opened my eyes to new fields in Biology to pursue in my future career. My spectrum of knowledge has expanded, not only in academia, but also in real life during our engaging conversations.

Furthermore, I would like to thank everyone who stood by me during my times of need, specifically Farah Ballout, who taught me all the lab procedures I have used for my research. Along with my lab members who were with me in every step, I greatly appreciate the continuous presence of my friends.

Finally, my biggest gratitude goes to my family who have always stood by me. They have always provided me with emotional support and comfort during my stressful periods. I am always encouraged to keep on moving forward and conquer obstacles because of them.

This thesis is dedicated to my everything, my Mom.

AN ABSTRACT OF THE THESIS OF

Rana Iyad Sarieddine for Master of Science
Major: Biology

Title: Anticancer Activity and Uptake Mechanisms of Thymoquinone-Loaded Cubosomal Nanoparticles in Human Breast Cancer

Background: Thymoquinone (TQ), the bioactive constituent of *Nigella sativa* (Black seed), exhibits anticancer potential, but its translation to the clinic is hindered by its hydrophobic property and poor bioavailability.
Nanoparticles (NP) are evolving as a therapeutic platform for cancer treatment. In this project, we encapsulated TQ in cubosomal nanoparticles and studied its anticancer effects *in vitro* and *in vivo*.

Methods: The TQ-loaded cubosomes were prepared by the emulsification technique. To study the cytotoxic and anticancer effects of the formulations, we performed MTT and trypan blue exclusion assays on human breast cell lines. These included the nontumorigenic MCF-10A mammary epithelial cells, the aggressive MDA-MB-231 and the MCF-7 breast cancer cell lines. These experiments were complemented with apoptosis assays in MDA-MB-231 cells by detecting caspase 3 cleavage and morphological changes in nuclei of treated cells by DAPI staining. Finally, the cell-NP interaction and the uptake of the formulation into the cells were investigated to determine their mode of entry and subcellular localization.
To determine whether TQ-loaded cubosomes confer an advantage over free TQ, 6 to 8-week-old female immunocompromised NSG mice (n=6 per group) were xenografted with MDA-MB-231 breast cancer cells. Once tumors were established, treatment started with blank cubosomes, or with 15 mg/kg of free TQ or its equivalent in TQ-loaded cubosomes. The body weight of mice and volume of tumors were measured three times/week and two animal experiments were performed. In the first experiment, treatment was administered intraperitoneally for 21 days. In the second experiment, treatment was administered subcutaneously to avoid the side effects of ascites formation that was observed with intraperitoneal injections.

Results: We observed a dose-dependent inhibitory response to treatment with TQ or TQ-loaded cubosomes in both breast cancer cell lines. According to MTT assay, at concentrations up to 30 μM, TQ-loaded cubosomes had a relatively non-cytotoxic effect on the MCF-10A non-tumorigenic cells reaching 77% viability at 30 μM. While TQ-NP was significantly more cytotoxic than free TQ on MCF-7 cells decreasing the viability dramatically by 70% at 30 μM, in comparison to a 30% decrease by free TQ. The activity of free TQ and TQ-NP against MDA-MB-231 cell line was approximately the same with the effect of TQ-NP being slightly greater. Trypan blue assay showed that the formulations had a less cytotoxic effect on MCF-7 cell line, a discrepancy that could be

explained by the fact that the MTT assay accounts for only the metabolically active cells. Quantification of the active caspase-3 (AC3) positive cells showed that free and encapsulated TQ significantly induced apoptosis in MDA-MB-231 cells, and this was coupled with an increase in the apoptotic bodies in the nuclei of the treated cells. Uptake studies showed that TQ-loaded cubosomes co-localized with caveolin, LAMP, EEA and transferrin labeling caveolae, lysosomes, early endosomes and clathrin coated pits, respectively.
In vivo the TQ-loaded cubosomes did not provide enhanced anticancer effects in both experiments. the first experiment, the tumor volume and the body weight of mice treated with TQ decreased significantly, while the tumor volume of those treated with blank cubosome or TQ-loaded cubosomes increased, in comparison to the control with evidence of serious side effects of mouse aggression and ascites formation. In experiment 2, the mice in all treatment groups showed a slight non-significant increase in tumor volume in comparison to control suggesting that subcutaneous injection is not an effective mode of administration.

Conclusion: TQ-loaded cubosomes appear to be a better system of drug delivery than free TQ against breast cancer *in vitro*. However, *in vivo*, the tested routes of administration did not seem to allow the drug to reach the targeted tissue which explains the lack of antitumor efficacy. Future studies should focus on identifying better routes of administering TQ-loaded cubosomes in mice.

CONTENTS

ACKNOWLEDGEMENTS..... v

ABSTRACT..... vi

LIST OF ILLUSTRATIONS..... xi

LIST OF TABLES..... xiv

LIST OF ABBREVIATIONS..... xv

Chapter

I. LITERATURE REVIEW..... 1

A. Overview 1

B. Breast Cancer: Types and Risk Factors 2

a) Cell Culture Model..... 4
b) Animal Model..... 5
c) Treatment of Breast Cancer..... 6

C. Thymoquinone..... 7

a) Thymoquinone Use Against Breast Cancer..... 9
b) Clinical Trials and Challenges for Translating TQ..... 11

D. Nanoparticles: Types and Targeting Mechanisms..... 12

a) Targeting Mechanisms of Nanoparticles..... 12
b) Translation of TQ-NPs to the Clinic 17
c) Uptake Mechanisms of Nanoparticles 17

II. HYPOTHESIS AND AIMS..... 19

III. EXPERIMENTAL PROCEDURE..... 24

A. Materials 24

B. *In vitro* experiments…… 24

1. Cell culture…… 24
2. Viability assay…… 25
3. Active caspase-3 immunofluorescence…… 26
4. Cellular uptake…… 27
5. Subcellular localization…… 27

C. *In vivo* experiment…… 28

1. Hematoxylin and Eosin staining…… 29
2. Cellular uptake…… 29
3. Immunohistochemistry…… 30

D. Statistical analysis…… 30

IV. RESULTS…… 31

A. Anticancer potential of TQ-loaded cubosomes…… 31

1. TQ-loaded cubosomal nanoparticles are equally or more cytotoxic to breast cancer cell lines than free TQ and are nontoxic to nontumorigenic breast cells…… 31
2. Free TQ and TQ-loaded cubosomes induce apoptosis in MDA-MB-231 through caspase-3 cleavage…… 37

B. Mechanism of cellular uptake of TQ-loaded cubosomal nanoparticles…… 39

1. Internalization of TQ-loaded cubosomes by MCF-7 and MDA-MB-231 cell lines…… 39
2. Mechanisms of cellular uptake of cubosomes into MCF-7 and MDA-MB-231 cell lines …… 41

C. Anticancer activity of intraperitoneally administered TQ-loaded cubosomes in breast cancer xenograft models…… 48

1. Hematoxylin and Eosin staining of tumor tissues 51
2. Cellular uptake of cubosomal nanoparticles in mice (experiment 1) …… 52
3. PCNA expression in mouse tumors by immunohistochemistry…… 54

D. Anticancer activity of subcutaneously administered TQ-loaded cubosomes in breast cancer xenograft models…… 56

1. Hematoxylin and Eosin staining of tumor tissues 58
2. Cellular uptake of cubosomal nanoparticles in mice (experiment 2) …… 59
3. PCNA expression by immunohistochemistry…… 61

V. DISCUSSION…… 63

VI. BIBLIOGRAPHY…… 73

ILLUSTRATIONS

Figure		Page
1.	Thymoquinone targets nine of the ten hallmarks of cancer……	8
2.	Passive and active targeting mechanisms of nanoparticles……	13
3.	MTT assay showing the viability of MCF-10A cell line after 24 h of treatment with different concentrations of either TQ, or blank NP or TQ-NP……	33
4.	MTT assay showing the viability of MCF-7 cell line after 24 h of treatment with different concentrations of either TQ, or blank NP or TQ-NP……	34
5.	MTT assay showing the viability of MDA-MB-231 cell line after 24 h of treatment with different concentrations of either TQ, or blank NP or TQ-NP……	35
6.	Trypan blue exclusion test showing the viability of MCF-7 cell line after 24 h of treatment with different concentrations of either TQ, or blank NP or TQ-NP……	36
7.	Trypan blue exclusion test showing the viability of MDA-MB-231 cell line after 24 h of treatment with different concentrations of either TQ, or blank NP or TQ-NP……	37
8.	Immunofluorescent analysis of active caspase-3 (AC3) expression in MDA-MB-231 cell line after 24 h of treatment with TQ and TQ-loaded cubosomes using the IC_{50} values obtained from MTT assay……	39
9.	Active caspase-3 quantification in MDA-MB-231 cell line treated for 24 h with TQ and TQ-loaded cubosomes at the IC_{50} values obtained from MTT assay……	40
10.	Cellular uptake of the formulations by MCF-7 cell line after 30 mins of treatment with the IC_{50} values obtained from MTT……	41
11.	Cellular uptake of the formulations by MDA-MB-231 cell line after 30 mins of treatment with the IC_{50} values obtained from MTT……	42

12. Immunofluorescent images of untreated cells (control), labeled with DAPI, LAMP and Caveolin…… 43

13. Immunofluorescent images of untreated cells (control), labeled with DAPI, EEA-1 and Transferrin…… 44

14. Subcellular localization of blank cubosomes labeled with Nile red in MCF-7 and MDA-MB-231 cell lines…… 45

15. Subcellular localization of blank cubosomes labeled with Nile red in MCF-7 and MDA-MB-231 cell lines…… 46

16. Subcellular localization of TQ-loaded cubosomes labeled with Nile red in MCF-7 and MDA-MB-231 cell lines…… 47

17. Subcellular localization of TQ-loaded cubosomes labeled with Nile red in MCF-7 and MDA-MB-231 cell lines…… 48

18. Graph showing the variation in the body weight of the 4 groups of mice (measured 3 times/week) as a function of time (days). Treatment was given intraperitoneally…… 50

19. Graph showing the variation in the tumor volume of the 4 groups of mice (measured by vernier caliper, 3 times/week) as a function of time (days). Treatment was given intraperitoneally…… 51

20. Mouse treated with blank cubosomes showing fluid retention in the area of intraperitoneal injection…… 51

21. Mice at day 21, day of sacrifice, after treating them intraperitoneally with either the vehicle, or blank cubosome, or 15 mg/kg TQ or its equivalent in TQ-loaded cubosomes…… 52

22. Hematoxylin and Eosin (H&E) staining of tumor tissues from mice treated intraperitoneally…… 53

23. Cellular uptake of cubosomes and TQ-loaded cubsosmes into cells in mice treated intraperitoneally…… 54

24. Immunohistochemistry analysis of PCNA expresssion in tumor tissues from mice treated intraperitoneally…… 56

25. PCNA expression (AU) in kidney, liver and tumor from mice treated intraperitoneally…… 57

26. Graph showing the variation of the body weight of the 4 groups of mice (measured 3 times/week) as a function of time (days), treated subcutaneously…… 58

27. Graph showing the variation of the tumor volume of the 4 groups of mice (measured by vernier caliper, 3 times/week) as a function of time (days), treated subcutaneously…… 58

28 Mice at day 21, day of sacrifice, after treating them subcutaneously… 59

29 Hematoxylin and Eosin (H&E) staining of tumor tissues from mice treated subcutaneously…… 60

30 Cellular uptake of cubosomes and TQ-loaded cubosomes into the cells in mice treated subcutaneously…… 61

TABLES

Table		Page
1.	Treatment protocol of the first *in vivo* experiment……	22
2.	Treatment protocol of the second *in vivo* experiment……	22
3.	Calculated IC_{50} values (µM) from MTT assay and trypan blue exclusion test of free TQ and TQ-loaded cubosomes in both MCF-7 and MDA-MB-231 cell……	74

ABBREVIATIONS

AC3	Active caspase-3
Akt	Protein kinase B
ALL	Acute lymphoblastic leukemia
Bax	bcl-2-like protein 4
Bcl	B-cell lymphoma
BRCA1/2	breast cancer associated gene 1 and 2
BSA	Bovine serum albumin
CVD	Cardiovascular diseases
DAB	3,3'-Diaminobenzidine
DAPI	4′,6-diamidino-2-phenylindole
DCIS	Ductal carcinoma in situ
DFI	disease-free survival
DMSO	Dimethyl sulfoxide
EDTA	Ethylenediaminetetraacetic acid
EEA-1	Early endosome antigen 1
eEF-2K	Eukaryotic epidermal factor 2 kinase

EGF	Epidermal growth factor
EGFR	Epidermal growth factor receptor
EMT	Epithelial–mesenchymal transition
EPR	Enhanced permeability and retention effect
ER	Estrogen receptor
FBS	Foetal bovine serum
H&E	Haematoxylin and Eosin
HDAC	Histone deacetylases
HER2	human epidermal growth factor receptor 2
HPLC	High performance liquid chromatography
IDC	Invasive ductal carcinoma
ILC	Invasive lobular carcinoma
IL2	Interleukin 2
Lamp-1	Lysosomal-associated membrane protein 1
MTT	3-(4,5 Dimethylthiazol-2-yl)-2,5-diphenyltetrazolium bromide
NCL	Nanostructured lipid carriers
NFκB	Nuclear factor kappa-light-chain-enhancer of activated B cells
NP	Nanoparticle

NR	Nile red
OS	overall survival
PBS	Dulbecco’s phosphate-buffered saline horse serum
PCNA	Proliferating cell nuclear antigen
PEG	Polyethylene glycol
PI	Propidium iodide
PR	Progesterone receptor
Prkdc	DNA-dependent protein kinase
P/S	penicillin–streptomycin
Rag	Recombination activating genes 1 and 2 (1and Rag2) and
ROS	Reactive oxygen species
SEM	Standard error
SLN	Solid lipid nanoparticles
TB	Trypan blue
TNFα	Tumor necrosis factor
TQ	Thymoquinone
VEGF	Vascular endothelial growth factor

CHAPTER I

LITERATURE REVIEW

A. Overview:

Breast cancer is the most common type of cancer reported in women according to the World Health Organization. Depending on the cancer type and its severity, conventional therapy includes chemotherapy or radiotherapy, among others. Chemotherapy is the most widely used treatment for cancer; however, it leads to several side effects due to non-selectivity, systemic toxicity and development of drug resistance. Besides, conventional treatment limits the amount of the drug to the tumor due to non-targeted delivery. Therefore, researchers are looking for alternative treatments with potential activities against cancer that are less toxic such as naturally extracted compounds.

Along with its diverse pharmacological actions, thymoquinone -extracted from *Nigella sativa*-, is a promising anticancer molecule. However, its translation to the clinic is hindered by its hydrophobic property and poor bioavailability.

Researchers found that encapsulating poor water-soluble drugs into nanoparticles would protect them from degradation, enhance their stability, bioavailability and retention. In addition, these drug delivery systems can be specifically targeted to tumor tissues either actively through a conjugated ligand or in response to a stimulus. Therefore, it becomes possible to deliver the whole drug while limiting its side effects and systemic toxicities.

In the current project, we aimed to enhance the anticancer effect of thymoquinone through its encapsulation into cubosomal nanoparticles (NPs). In this

chapter, we describe the cancer model we used to investigate the anticancer potential of the TQ-loaded NPs. In addition, we elaborate on the anticancer activity of TQ, its promise and limitations and emphasize the importance of nano-formulations and their application in cancer treatment.

B. Breast Cancer: Types and Risk Factors

Cancer is one of the most distressing diseases, being the second leading cause of death with 18.1 million new cases and 9.6 million deaths in 2018 with no definite cure yet (World Health Organization). Cancer incidence and mortality are continuously increasing due to aging, growth of population, changes in the prevalence of the risk factors according to socioeconomic development (Bray, Ferlay et al. 2018). According to a recent statistical study, the estimated number of new cancer cases in the United States of America reached 1,762,450 in 2019 (Siegel, Miller et al. 2019).

According to the world region, one-half of the newly diagnosed cases and over one-half of deaths occurred in Asia in 2018, followed by Europe and then the Americas (Bray, Ferlay et al. 2018).

Female breast cancer ranks as the second leading cause of death worldwide, preceded by lung cancer, for males and females combined (Bray, Ferlay et al. 2018).

Breast cancer is the most common type of cancer reported in women, representing 30% of the newly diagnosed cancer cases, with a mortality estimate of about 15% of deaths in 2019 (Siegel, Miller et al. 2019).

Breast cancer incidence rate increased from 2006 to 2015 and this may be due to obesity and a decrease in parity (Cronin, Lake et al. 2018).

Several factors contribute to the development and pathogenesis of breast cancer. Hereditary and genetic factors play an important role in increasing the incidence rate by transmitting the genetic mutations associated with breast cancer. These include mutations in the breast cancer associated gene 1 and 2 (BRCA1/2) that encode tumor suppressor proteins, or in the human epidermal growth factor receptor 2 (HER2) which is a protooncogene, or in the epidermal growth factor receptor (EGFR), among others (Sun, Zhao et al. 2017). Other factors that contribute to the development of breast cancer include excessive alcohol and dietary fat intake, exogenous hormone intake, reproduction such as early menarche and late menopause while breastfeeding and physical activity lowers the risk of breast cancer (Sun, Zhao et al. 2017, Bray, Ferlay et al. 2018).

The breast is composed of lobes that in turn are formed of multiple lobules. These lobules, formed of alveoli which are the basic components of the mammary gland, connect to a terminal interlobular duct carrying milk to the nipples. The lobules and ducts are surrounded by a layer of luminal epithelial cells followed by myoepithelial cells that are separated from the stroma by a basement membrane. The stroma comprises the extracellular matrix, adipocytes, immune cells, blood vessels, among others (Bertos and Park 2011).

Breast cancer is a heterogeneous disease containing several clonal subpopulations that express different biomarkers in different proportions (Bertos and Park 2011). Breast cancer is divided into several types based on different criteria which include the histological type, immunopathology, histological grade, and the gene expression level; with histological type and immunopathology being the most recognized criteria (Weigelt, Geyer et al. 2010, Bertos and Park 2011). According to the

structural heterogeneity, the most common type of breast cancer is the invasive ductal carcinoma (IDC) accounting for about 75% of the cases, followed by the invasive lobular carcinoma (ILC) and the breast cancer special types accounting each for about 10% of the cases (Weigelt, Geyer et al. 2010, Bertos and Park 2011). Ductal carcinoma in situ (DCIS) is the immediate precursor of the invasive breast cancers (Allred 2010). They are further divided into subtypes according to the expression of certain biomarkers, specifically the estrogen receptor (ER), progesterone receptor (PR), and human epidermal receptor 2 (HER2). The subtypes are ER+ (ER+/HER2–), HER2+ (ER–/HER2+), triple negative (TN; ER–/PR–/HER2–), and triple positive (ER+/PR+/HER2+) breast cancers (Bertos and Park 2011). The ER+ cancers are divided into two luminal subtypes (A and B) where they differ in the expression of ER-regulated genes (Bertos and Park 2011).

a) Cell Culture Model

The *in vitro* culture models that are commonly used to study the human breast tissue in its normal and diseased state have limitations. MCF-10A human breast cell line is the generally used cell line to represent the normal mammary tissue; however, one study questioned the suitability of this model (Qu, Han et al. 2015). MCF-10A breast cell line resembles the normal breast epithelium by being anchorage-dependent and forming acinar structure in 3D culture (Qu, Han et al. 2015). In 2D culture, this cell line expressed some markers for luminal, basal and mesenchymal cell types (CK5, CK17, SMA, vimentin and CK8); however, it lacked the expression of other essential markers (CK14, P63, CK7, Muc1 and CK18). MCFA-10A cell line was previously classified as

a basal-type mammary epithelial cell line, but a study has shown that this cell line possesses several cell types (Qu, Han et al. 2015).

MCF-7 breast cancer cell line has been used for over 45 years in research, specifically for testing anticancer drugs, since it mimics several human breast cancers. MCF-7 cell line belongs to luminal A subtype expressing epithelial markers, and estrogen and progesterone receptors. This cell line is non-metastatic, unlike MDA-MB-231 breast cancer cell line, since it expresses low levels of the vascular endothelial growth factor (VEGF) (Comsa, Cimpean et al. 2015, Lee, Oesterreich et al. 2015). MDA-MB-231 cancer cell line is a triple negative cell line, commonly used to study the metastatic human breast cancer system (Liu, Newbury et al. 2019). Due to its aggressiveness and mimicry to the human breast cancer, MDA-MB-231 xenograft model in mice is the widely used model to investigate breast cancer pathogenesis *in vivo*. MDA-MB-231 cell line exhibits higher expression levels of EGFR, in comparison to MCF-7 cell line. EGFR activation stimulates the PI3K/AKT/mTOR pathway which, in turn, activates the Warburg effect (aerobic glycolysis) by regulating the glucose transporter GLUT1 and the cytoskeletal dynamics (Makinoshima, Takita et al. 2015, Manupati, Dhoke et al. 2017). Therefore, MDA-MB-231 cell line depends on glycolysis more than MCF-7 cell line does (Reda, Refaat et al. 2019).

b) Animal Model

Due to certain limitations in the two-dimensional *in vitro* model, tumorigenicity should be investigated in *in vivo* models. *In vitro* models disregard *in vivo* conditions, including the tumor microenvironment, vascularization and the

immunologic environment. Therefore, in order to study tumor pathogenesis, researchers developed immunocompromised mice that lack the innate and adaptive immune system to be able to xenograft human-derived cancer cells. NOD-Prkdc^{scid} IL2rg^{null} (NSG) mice are one of the most immunodeficient mice lacking both the innate and adaptive immunity (Shultz, Goodwin et al. 2014). NSG mice have spontaneous mutations in protein kinase DNA activated catalytic polypeptide (Prkdc) and targeted mutations in recombination activating genes 1 and 2 (Rag1and Rag2) and IL2 receptor common gamma chain gene (IL2rγ) (Shultz, Goodwin et al. 2014).

c) Treatment of Breast Cancer

Depending on the breast cancer type and its severity, conventional treatment of breast cancer includes chemotherapy, radiotherapy, surgery, endocrine therapy and targeted therapy. Surgery is performed for localized breast cancer, preceded by neoadjuvant therapy and followed by adjuvant therapy to prevent secondary tumor growth (Matsen and Neumayer 2013, Nounou, ElAmrawy et al. 2015). Endocrine therapy is administered in ER-positive patients to balance or block the hormones, while chemotherapy is most pronounced in ER-negative cases (Nounou, ElAmrawy et al. 2015). However, conventional therapy leads to several side effects which affect the disease-free interval (DFI) and overall survival (OS) (Bodai and Tuso 2015). Adjuvant therapies increase the risk of cardiovascular diseases (CVD), thus increasing the risk of death in breast cancer survivors due to CVD. Most chemotherapeutic drugs lead to chronic cardiovascular complications, including congestive heart failure, hypertension, and bradycardia (Bovelli, Plataniotis et al. 2010, Bodai and Tuso 2015). Radiotherapy

leads to skin problems, damage to the myocardium and coronary arteries (Akram and Siddiqui 2012, Bodai and Tuso 2015). The most important example of hormonal modulators, Tamoxifen, leads to depression, mood swings, thromboembolic complications, and an increase in endometrial cancer risk (Bodai and Tuso 2015).

The most widely used treatments for cancer lead to several side effects due to non-selectivity, high-dose requirement, poor bioavailability and systemic toxicity. Therefore, researchers are looking for alternative less toxic treatments such as naturally extracted compounds with potential activities against cancer. One main advantage is that these natural compounds could be used in combination with lower doses of standard chemotherapy drugs to enhance their efficacy and lower their toxicity.

C. Thymoquinone

Nigella sativa, commonly known as the black seed, has been thoroughly studied over the years exhibiting many pharmacological actions through its main active constituent thymoquinone (TQ). TQ is a yellow crystalline molecule (2-methyl-5-isopropyl-1,4-benzoquinone), first identified in 1963 representing 54% of the volatile oil of the black seed, that has been used for 2000 years in traditional folk medicine (Schneider-Stock, Fakhoury et al. 2014). Immune system stimulatory, anti-inflammatory, hypotensive, hepatoprotective, anticancer and hypoglycaemic properties of TQ were previously reported. Focusing on its anticancer effect, TQ was shown to modulate nine of the ten hallmarks of cancer (Figure 1), among which is the prevention of cancer cell evasion from growth suppressors (Gali-Muhtasib, Abou Kheir et al. 2004, Li, Rajendran et al. 2010, Subburayan, Thayyullathil et al. 2018), cell cycle arrest at

different phases and growth inhibition (Gali-Muhtasib, Diab-Assaf et al. 2004, Alhosin, Abusnina et al. 2010, Yang, Kuang et al. 2015, Kabil, Bayraktar et al. 2018), induction of apoptosis (Das, Dey et al. 2012, Dastjerdi, Mehdiabady et al. 2016, Samarghandian, Azimi-Nezhad et al. 2018), inhibition of vascular endothelial growth factor (VEGF) thus exhibiting anti-angiogenic and anti-inflammatory effects by inhibiting the pro-inflammatory mediators including TNFα and NFκB (Li, Rajendran et al. 2010, Zhang, Bai et al. 2016).

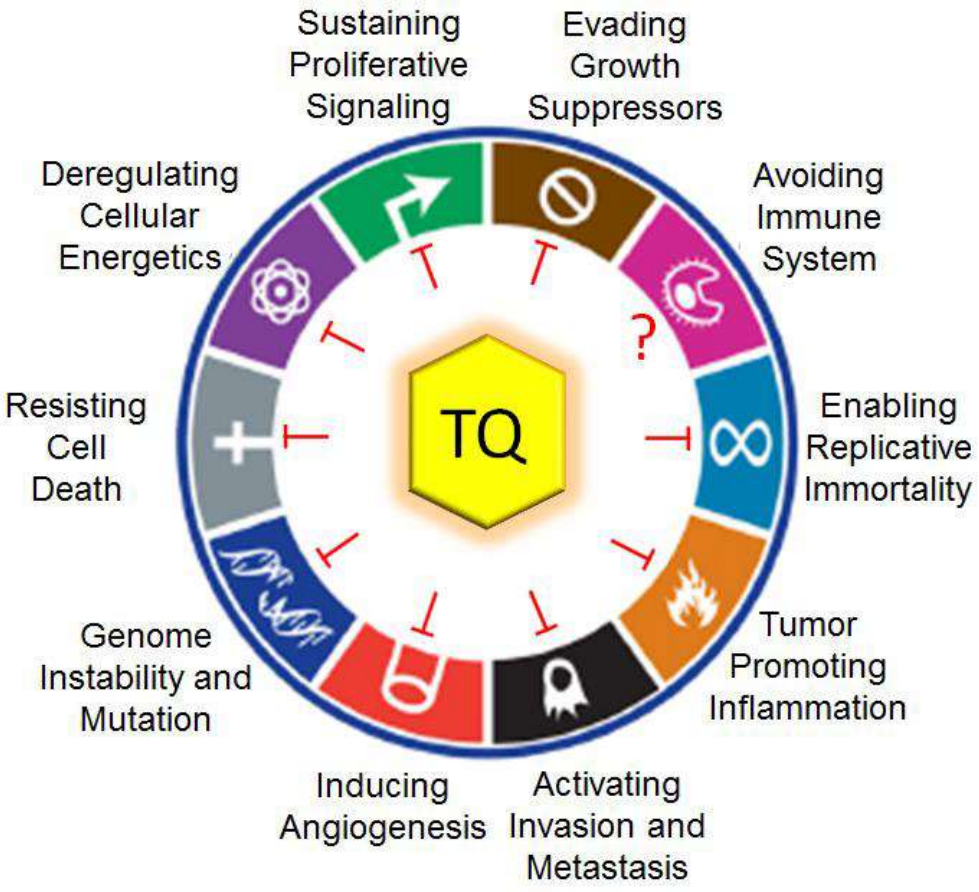

Figure 1. Thymoquinone targets nine of the ten hallmarks of cancer (Reproduced with permission from Schneider-Stock et al., 2014, Drug Discovery Today, Vol. 19, 18-30).

a) Thymoquinone Use Against Breast Cancer

The anti-proliferative and pro-apoptotic effects of TQ were shown against MDA-MB-468 and T-47D cell lines. These effects were accompanied by the inhibition of cyclin D1, cyclin F, cyclin dependent kinases and AKT, and the impairment of the mitochondria (Rajput, Kumar et al. 2013). Another study showed that TQ induces apoptosis in MCF7 cells, in a time-dependent manner, through the upregulation of p53 protein (Dastjerdi, Mehdiabady et al. 2016). In addition, TQ inhibited the invasion and growth of MDA-MB-231 and MCF-7 cell lines through the inhibition of AKT phosphorylation, leading to DNA damage and activation of the mitochondrial apoptotic pathway (Attoub, Sperandio et al. 2013).

The most aggressive and chemo-resistant subtype of cancer is the triple-negative breast cancer (TNBC) exhibiting poor prognosis and survival due to the overexpression of the eukaryotic epidermal factor 2 kinase (eEF-2K) (Hamurcu, Ashour et al. 2016). It was shown that TQ inhibits the mRNA and protein expression of eEF-2K, its downstream targets, and NF-κB thus inducing the tumor suppressor miR-603. These effects led to a decrease in the proliferation, migration and invasion of TNBC(Kabil, Bayraktar et al. 2018). Similar effects were shown in another study where TQ decreased the transcriptional activity of TWIST1 promoter, an EMT-promoter transcription factor, controlling the expression of TWIST1-regulated genes in MDA-MB-435 and BT549 cell lines (Khan, Tania et al. 2015).

The activity of chromatin, determined by the acetylation/deacetylation state, regulates many cellular activities (Glozak and Seto 2007). Histone deacetylases

(HDAC) were shown to silence genes involved in the cell cycle, and most of the FDA approved HDAC inhibitors have side effects (Glozak and Seto 2007, Azad, Zahnow et al. 2013). A study showed that TQ attenuates HDAC activity by regulating the activity of its downstream genes specifically by the activation of Bax gene, a pro-apoptotic gene, and the downregulation of Bcl-1 gene, an anti-apoptotic gene, and arresting the cell cycle at G2/M phase leading to the inhibition of metastasis (Parbin, Shilpi et al. 2016).

TQ's effects have been extensively tested in animal models. The administration of TQ in nude mice xenografted with human breast cancer cells (MDA-MB-231 cell line) inhibited tumor growth due to the inhibition of the protein expression of the anti-apoptotic genes XIAP, survivin, Bcl-xL and Bcl-2 as well as the production of the antioxidant enzymes catalase, superoxide dismutase and glutathione leading to p38 phosphorylation (Woo, Hsu et al. 2013). A study investigating TQ's effect on the metastasis of breast cancer to bone, *in vitro* and *in vivo*, showed that TQ inhibited CXCR4 expression, a tumor metastasis promoting molecule, in both MCF-7 and MDA-MB-231 cell lines. In addition, TQ inhibited tumor growth and reduced metastasis, in a breast cancer animal model, due to a significant reduction in CXCR4, Ki67, MMP9, VEGFR2 and COX2 expression (Shanmugam, Hsu et al. 2016, Shanmugam, Ahn et al. 2018).

Besides its promising anti-cancer effects against almost all cancer types and specifically against breast cancer, TQ could be considered as an inexpensive, readily available drug from plants that is non-toxic to normal cells and tissues and thus is worth translating to the clinic.

b) Clinical Trials and Challenges for Translating TQ

Thymoquinone was tested clinically and it was shown that it is safe showing no or minor side effects. However, most of the studies were carried out to test TQ's effect against diseases other than cancer, including diabetes, inflammation, metabolic syndrome, cardiovascular diseases, among others.

A study by Dogar *et al* showed that when L-asparaginase was substituted by *Nigella sativa* powder (40 mg/kg in two equal doses for 3 months), along with the conventional therapy in children with acute lymphoblastic leukemia (ALL), less side effects were reported (Asaduzzaman Khan, Tania et al. 2017). However, when TQ was given orally (starting dose level of 3, 7, or 10mg/kg/day) to adult patients with solid tumors that failed or relapsed conventional treatment, neither side effects nor anticancer effects were seen. There are no clinical trials for thymoquinone registered in the U.S government yet. However, in an Arabian phase I clinical trial on terminal cancer patients, thymoquinone was found to be safe up to 10 mg/kg/day without showing a significant anticancer effect (Asaduzzaman Khan, Tania et al. 2017).

Besides TQ's physiological importance, it has certain limitations that restricted it from reaching the clinic. These include its hydrophobic nature and reduced solubility and bioavailability (Jain 2000), in addition to its strong ability to bind plasma proteins, thus reducing the amount that should reach the tumor site (El-Najjar, Ketola et al. 2011). Pharmacokinetic studies showed that thymoquinone exhibits low bioavailability due to rapid elimination and slow absorption (Alkharfy, Ahmad et al. 2015, Asaduzzaman Khan, Tania et al. 2017).

D. Nanoparticles: Types and Targeting Mechanisms

To enhance the drug's bioavailability and solubility property, researchers have found that encapsulating drugs into nanoparticles is the solution. Due to their physical characteristics of having a diameter between 10 and 100 nm, according to the National Cancer Institute for cancer cell targeting, and a large surface-to-volume ratio, nanoparticles (NPs) form a suitable drug delivery system. Nanoparticles with diameters less than 10 nm are susceptible to renal clearance and tissue extravasation, and NPs with diameters greater than 100 nm are prone to opsonisation by macrophages (Souza 2014). Nanoparticles serve as a cargo for the drugs having the ability to cross cell and tissue barriers, control the release rates, protect the drug from non-specific binding and degradation, thus enhancing its bio-distribution, bioavailability and retention (Kumari, Yadav et al. 2010, Wang, Langer et al. 2012, Souza 2014, Petschauer, Madden et al. 2015). In addition, each NP will carry more than one drug molecule, thus increasing the concentration of the drug delivered to the tumor site without affecting normal tissues.

a) Targeting Mechanisms of Nanoparticles

Drugs can be delivered to the targeted tissue *via* one of the two targeting mechanisms, either passively or actively. Since highly aggressive tumors form fenestrated vasculature having deregulated and leaky nature with poor lymphatic drainage near the tumor sites, the NPs will be retained and will accumulate near the tumor sites thus decreasing their exposure to normal tissues and reducing side effects.

This enhanced permeability and retention effect (EPR) results in passive drug targeting to the tumors which ensures an advantage for NP encapsulated drugs over free drugs (Siemann 2011, Viallard and Larrivee 2017). To provide further specificity, drugs can be delivered by active targeting where an overexpressed receptor or ligand on the target cell surface is identified and a specific and selective targeting agent(s) is coupled to the NP surface triggering receptor endocytosis, avoiding non-specific interactions and localization of the drug in peripheral tissues, thus lowering systemic toxicity (Bazak, Houri et al. 2015). Therefore, both targeting mechanisms provide enhanced localization of the drug; however, active targeting provides enhanced uptake and internalization *via* receptor-mediated endocytosis (Bazak, Houri et al. 2015).

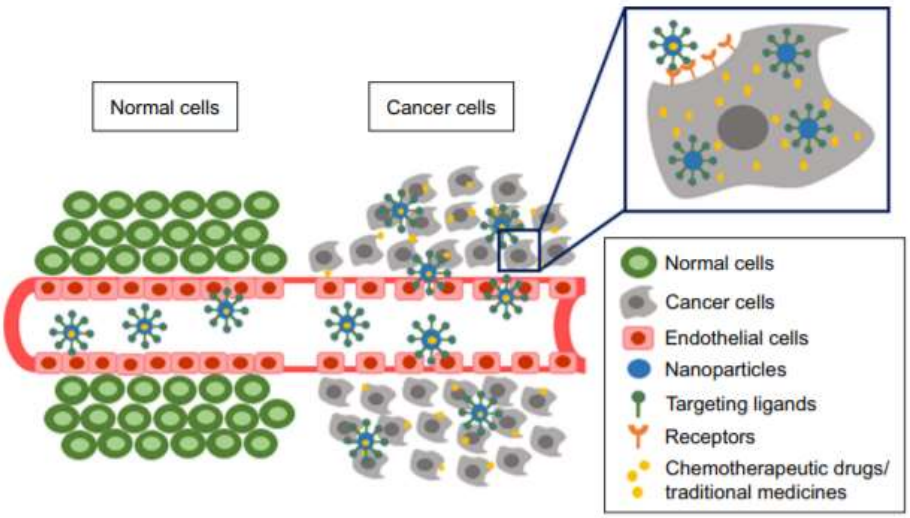

Figure 2. Passive and active targeting mechanisms of nanoparticles (Reproduced with permission from Muhamad et al., 2018, International Journal of Nanomedicine, Volume 13, 3921-3935).

Nanoparticles can be either organic or inorganic. Thymoquinone has been encapsulated in both NP types, but mostly in organic ones. Examples of organic NPs

and their importance in cancer therapy in general and breast cancer specifically will be discussed next. Most commonly used NPs for drug encapsulation are lipid-based NPs and polymeric NPs.

Organic nanoparticles:

1. Lipid-based nanoparticles:

Liposomes: they are the classical lipid-based nanoparticles. They are artificial vesicles formed of an amphiphilic phospholipid bilayer surrounding an aqueous core. They are biocompatible and biodegradable, and can encapsulate hydrophilic and hydrophobic drugs; however, they are rapidly cleared from the bloodstream (Ballout, Habli et al. 2018, Senapati, Mahanta et al. 2018).

Thymoquinone was encapsulated in liposomes (TQ-loaded liposomes) and an enhancement of TQ's anticancer activity was reported, on MCF-7 and T47D breast cancer cell lines, while maintaining its stability, improving its bioavailability and showing no toxicity to normal fibroblasts (Odeh, Ismail et al. 2012).

Solid lipid nanoparticles (SLN): to enhance drug delivery, release and stability, researchers developed non-phospholipid-based NPs. SLNs protect sensitive molecules, improve the bioavailability and the controlled release profile of the drugs (Das and Chaudhury 2011). The release profile of TQ, once encapsulated in SLNs, is biphasic; characterized by an initial rapid release followed by a slower controlled one (Pathan, Jain et al. 2011). A study showed a two-fold increase in bioavailability of TQ-SLN, in

comparison to free TQ, thus increasing plasma concentration and retention in rats when administered orally (Pathan, Jain et al. 2011).

Nanostructured lipid carriers (NCLs): NCL is also a colloidal lipid-based nanoparticle formed of incompatible solid and liquid lipids having higher entrapment efficiency and drug loading capacity (Ballout, Habli et al. 2018). TQ-NCL, when tested on breast cancer cells (MCF-7 and MDA-MB-231) and cervical cancer cell lines (HeLa and SiHa), inhibited their growth in a dose-dependent manner by inducing cell cycle arrest followed by apoptosis (Ng, Saiful Yazan et al. 2015).

Cubosomes: cubosomes are self-assembled lipid liquid-crystalline nanostructures. The main precursor is monoolein formed of a mixture of glycerides and other fatty acids. Cubosomes have bicontinuous lipid cubic phases formed of three dimensional lipid bilayers with pores formed by interwoven water channels, which allows it to encapsulate hydrophobic, hydrophilic and amphiphilic compounds (Nazaruk, Majkowska-Pilip et al. 2017). Cubosomes are a promising drug delivery system since they confer advantage over other NP types by possessing better stability, high surface area to volume ratios (i.e. high loading capacity), and a large hydrophobic volume that allows encapsulating higher amount of poor water-soluble drugs (Murgia, Bonacchi et al. 2013, Mohyeldin, Mehanna et al. 2016, Nazaruk, Majkowska-Pilip et al. 2017). In addition, cubosome encapsulation of drugs reduces their rapid clearance from the bloodstream and enhances their physical and chemical stability (Barreto, O'Malley et al. 2011, Nazaruk, Majkowska-Pilip et al. 2017). Most importantly, they are pH-responsive carriers that do not release the loaded drug except in acidic environments, which is the common microenvironment in tumor sites, thus increasing selectivity and

decreasing systemic toxicity (Kluzek, Tyler et al. 2017, Nazaruk, Majkowska-Pilip et al. 2017).

2. Polymeric nanoparticles:

Polymeric NPs are solid colloidal systems; safe, biodegradable and biocompatible. Most importantly, they are stable in the blood. They can be structurally modified during synthesis to achieve the optimal drug loading capacity and bio-distribution (Ballout, Habli et al. 2018, Senapati, Mahanta et al. 2018). Encapsulation of TQ in polyethylene glycol (PEG) nanoparticles enhanced its cytotoxic effects while being less toxic to normal cells in comparison to free TQ. In addition, PEG-TQ-NPs exhibited anti-migratory effects on breast cancer cell lines through depolymerisation of actin due to miR-34a upregulation in a p53-dependent manner (Bhattacharya, Ahir et al. 2015).

3. Dendrimers:

Dendrimers form suitable cargos for water insoluble drug delivery due to their physicochemical characteristics, including biocompatibility, biodegradability, water solubility, size uniformity and high surface area (Senapati, Mahanta et al. 2018).

Encapsulation of TQ in dendrimers enhanced its stability and release profile. In addition, its anticancer potential was improved by enhancing the cytotoxicity of TQ on MDA-MB-231 breast cancer cell line and increasing ROS levels and disrupting the mitochondrial membrane potential leading to apoptosis (Mistry et al. 2016).

b) Translation of TQ-NPs to the Clinic

Several nanoparticle types are so far FDA approved and others are currently being tested in phase I and II clinical trials. However, none of the TQ-loaded nanoparticle formulations have reached the clinic due to the lack of toxicological studies and the inefficiency in synthesizing large batches of the formulation with the recommended size (Ballout, Habli et al. 2018). Nevertheless, several NP formulations encapsulating naturally derived compounds that share common characteristics with TQ have been FDA approved. Some of these formulations, in relevance to breast cancer, are pegylated liposome doxorubicin and Methoxy-PEG-poly (D, L-lactide) Taxol (Ballout, Habli et al. 2018).

Among the lipid-based NPs, only liposomes have been FDA approved. The lipid-based pegylated liposome doxorubicin and the polymeric Methoxy-PEG-poly (D, L-lactide) Taxol formulations increased the concentration of the drug to the target tissues while increasing the tolerability and decreasing side effects (Wang, Langer et al. 2012, Ballout, Habli et al. 2018).

c) Uptake Mechanisms of Nanoparticles

Several factors affect the uptake mechanisms of nanoparticles into the cell including the physicochemical characteristics of the NP (size, surface charge and area, shape, etc.), receptors involved, tumor microenvironment, among others. Nanoparticles mainly enter the cell through endocytosis, where the NPs are engulfed in membrane invaginations and then pinched off to form endocytic vessels to be transported to

intracellular trafficking compartments. NPs usually follow one of the five routes of endocytosis, including phagocytosis, clathrin-mediated endocytosis, caveolin-mediated endocytosis, clathrin/caveolae-independent endocytosis, and micropinocytosis (Behzadi, Serpooshan et al. 2017).

CHAPTER II

HYPOTHESIS AND AIMS

This project aimed to test the anticancer activity of a novel nanoparticle cubosomal formulation of TQ *in vivo* and *in vitro*. Self-assembled lipid cubosomal nanoparticles possess several characteristics that favor them over other nanoparticle types and allow them to serve as a suitable cargo. An enhancement of the activity of TQ cubosome nanoparticles due to enhanced targeting and retention is expected. We hypothesized that Thymoquinone encapsulated in cubosomes will show better anticancer effects against breast cancer compared to free TQ.

The project consisted of three specific aims:

1. Formulation of thymoquinone loaded self-assembled cubosomal nanoparticles and studying their physicochemical characteristics.

Cubosomal nanoparticles have been already prepared by Dr. Mohammed Mehanna (Associate Professor of Pharmaceutical Technology, Beirut Arab University, Lebanon). So, we grouped efforts with Dr. Mehanna to test the anticancer activity of this formulation *in vitro* and *in vivo*.

The particle size and polydispersity indices of TQ-loaded cubosome formulation were determined using photo correlation zeta sizer obtained at a fixed angle of 90º at 25 ±0.5ºC. To ensure physical stability of the TQ-NP dispersion, zeta potential

measurements were determined using milli Q distilled water placed in an electrophoretic cell at an average electric field of about 15V/cm using Malvern dispersion technology software. To quantify the amount of thymoquinone encapsulated in the formed cubosomes, encapsulation efficacy was measured by HPLC.

2. Investigation of the anticancer potential and the possible mechanisms of cellular uptake of the TQ-cubosome platform.

The cytotoxicity of the TQ-loaded cubosome formulation was investigated in nontumorigenic MCF-10-A human breast cells; while the uptake, distribution, as well as the anticancer potential were investigated in MCF-7 and MDA-MB-231 human breast cancer cells. MTT assay and trypan blue exclusion test were used to determine the inhibitory effect of TQ, TQ-loaded cubosomes, and blank NPs on the viability of these cell lines.

To study the cellular uptake and subcellular localization of TQ-loaded cubosomes *in vitro*, Nile red (NR) fluorescent dye was incorporated into the NP formulation. Uptake of fluorescent TQ-loaded cubosomes was determined qualitatively by confocal microscopy.

The apoptotic effect of the TQ-loaded cubosomes was assessed in MDA-MB-231 cells by microscopic imaging of the apoptotic bodies and quantification of the active form of caspase-3.

3. Evaluation of the anticancer activity of free TQ and TQ-loaded cubosomes formulation *in vivo* and study of the involvement of key signalling molecules in influencing tumor response.

The activity of the TQ-loaded cubosome in animal models was assessed to determine whether the formulation confers an advantage over free TQ. Given that *in vivo* highly aggressive tumors form fenestrated vasculature, we expect to observe enhanced NPs effects due to an increase in tumor targeting which was tested by incorporating the formulations with the fluorescent dye, Nile Red, and visualizing them by fluorescent microscopy.

The anticancer effects of TQ and TQ-loaded cubosomes was determined in the immunocompromised NSG mice xenografted with MDA-MB-231 human breast cancer cells.

The experiment was performed on four groups of mice with six mice/group. The animal protocol was approved by The NUS Institutional Animal Care and Use Committee (IACUC No. 19-04-RN547). Breast cancer cells were injected subcutaneously into 4 to 6-week-old female NSG mice ($3*10^6$ cells resuspended in sterile physiologic NaCl solution). Tumor development was followed and size of tumor (width, length and height) was determined using Vernier callipers. Treatment started when tumors reached a mean diameter of approximately 7 mm (treatments protocols are summarized in the tables 1 and 2). 15 mg/kg of free TQ or its equivalent in TQ-loaded cubosomes were injected. When endpoint was reached, the animals were sacrificed, and tissues were fixed in neutral buffer formalin then embedded in paraffin and stored for

immunohistochemistry and histological analysis. All the sections were examined by light and fluorescent microscopy.

The *in vivo* experiment was repeated twice to test the effectiveness of different routes of administration of the TQ-loaded cubosomes. In the first experiment, the treatments were administered intraperitoneally for 21 days. In the second experiment, they were administered subcutaneously for the same period of time.

Table 1. Treatment protocol of the first *in vivo* experiment.

Group	Treatment	Number of Animals	Method of Delivery
1	Vehicle	6	Intraperitoneal injection (3 times/week)
2	Blank NP	6	Intraperitoneal injection (3 times/week)
3	Free TQ (15 mg/kg)	6	Intraperitoneal injection (3 times/week)
4	TQ-NP	6	Intraperitoneal injection (3 times/week)

Table 2. Treatment protocol of the second *in vivo* experiment.

Group	Treatment	Number of Animals	Method of Delivery
1	Vehicle	6	Subcutaneous injection (3 times/week)
2	Blank NP	6	Subcutaneous injection (3 times/week)
3	Free TQ (15 mg/kg)	6	Subcutaneous injection (3 times/week)
4	TQ-NP	6	Subcutaneous injection (3 times/week)

The fluorescent dye Nile red was incorporated into all the formulations to confirm the uptake of TQ-NPs into the cells.

Injection of tumor cells into mice causes distress (pain category D); however, the xenografts were resected when their volume reached approximately 1800 mm^3 (usually 25 days after injection) which is before tumors reached a size that would create tumor burden. Animals were anaesthetized with inhaled isoflurane and then sacrificed by cervical dislocation 21 days after initiation of the treatment.

Significance of the Study:

Breast cancer is the most reported type of cancer in women. Since chemotherapy leads to non-specific targeting and systemic toxicities, scientists are searching for potential alternative treatments including naturally extracted compounds, among which is thymoquinone (TQ) from *Nigella sativa*. TQ exhibits many pharmacological activities, most importantly anticancer potential; however, this activity is limited by its hydrophobic nature and its poor bioavailability. To overcome this limitation, we believe that its encapsulation in nanocarriers could be the solution. In this project, we encapsulated TQ in a novel nanoparticle cubosomal formulation. Cubosomes exhibit many properties that favour their use over other NP types. We expected that this formulation will have enhanced retention and bioavailability and thus enhanced anticancer activities.

This is the first study that tests this type of TQ formulation *in vitro* and *in vivo*. The project forms a platform for the discovery of a novel drug against breast cancer and its possible translation to the clinic. If this formulation proves to be effective against breast cancer, future studies are required to investigate its effects on the signalling pathways and the key molecules it targets.

Chapter III

Experimental Procedure

A. Materials

Dulbecco's Modified Eagle Medium (DMEM) and DMEM-F12 cell culture media were purchased from Lonza (Verviers, Belgium). Thymoquinone, trypsin–EDTA, Dulbecco's phosphate-buffered saline (PBS), horse serum, foetal bovine serum (FBS), penicillin–streptomycin (P/S), epidermal growth factor, hydrocortisone, insulin, cholera toxin, DMSO, MTT (3-(4,5 Dimethylthiazol-2-yl)-2,5-diphenyltetrazolium bromide), trypan blue and methanol were purchased from Sigma Aldrich (St Louis, Missouri, USA). DAPI stain was purchased from Abcam (Cambridge, UK). Caveolin 1N-20 rabbit polyclonal, transferrin H-65 rabbit polyclonal, EEA-1 E-8 mouse monoclonal IgG, and lamp-1 H4A3 mouse monoclonal IgG antibodies were purchased from Santa Cruz Biotechnology (Paso Robles, California, USA). Cleaved caspase-3 monoclonal antibody was purchased from Cell Signalling Technology (Danvers, Massachusetts, USA).

B. *In vitro* experiments

1. Cell culture

MCF-10A normal breast cells were grown in DMEM/F-12 cell culture media supplemented with 1 % penicillin/streptomycin (P/S with penicillin at 10,000 units and streptomycin at 10 mg/ml), 5 % horse serum, 20 ng/ml epidermal growth factor, 0.5 mg/ml hydrocortisone, 100 ng/ml cholera toxin, and 10 µg/ml insulin. MDA-MB-231 breast cancer cells were grown in DMEM cell culture media supplemented with 10 % heat-inactivated FBS and 1% penicillin and streptomycin. MCF-7 breast cancer cells were grown in DMEM cell culture media supplemented with 10 % heat-inactivated FBS, 1% P/S, 5% sodium pyruvate and 5% non-essential amino acids. All cells were maintained in a humidified atmosphere of 5 % CO_2 at 37 ºC.

2. Viability assay

Viable cells have the ability to reduce the MTT (3-(4,5-Dimethylthiazol-2-yl)-2,5-diphenyltetrazolium bromide) dye, a yellow tetrazole, into a purple insoluble formazan product the absorbance of which is recorded at 595 nm. MTT assay was used to determine the inhibitory effect of TQ, TQ-loaded cubosomes, and blank cubosomes on the viability of MCF-7 and MDA-MB- 231 breast cancer cells and nontumorigenic MCF-10A breast cell line. Cells were seeded in 96-well plates at a density of 10,000 cells well. TQ was dissolved in methanol and then diluted in respective media. Loaded and unloaded cubosomes were diluted in respective media. All treatments were performed at 50 % confluency. At 24 h after treatment, the medium was removed and the cells were incubated for 3 hours with MTT solution (1 mg/ml prepared in PBS). After 3 hours, the solution containing the MTT dye was removed and replaced by isopropanol to dissolve the formazan crystal prior to measuring the colorimetric

absorbance of the different wells at 595 nm using a microplate reader. Cellular viability was expressed as percentage of cell viability of treated cells relative to untreated controls.

Cell viability was also determined by Trypan Blue Exclusion Test. Following treatment of cells for 24 hours, live and dead cells were collected. Samples were then centrifuged at 1500 rpm for 5 min. Pellets were resuspended in growth medium. TB was added to the cell suspension. Cells were counted using a haemocytometer under a light microscope. Cells stained blue were counted as dead, and results were expressed as a percentage of total cells. Experiments were performed at least three times.

3. Active Caspase-3 immunofluorescence

Cells were plated on cover slips in 12 well plates at a density of 60,000 cells/ml of MDA-MB-231 cells. After overnight incubation in 1 ml of respective growth medium, the medium was removed and the cells were treated for 24 h with either TQ, or blank cubosomes, or NR-TQ-loaded cubosomes. After treatment, the cells were washed twice with PBS and fixed at room temperature for 20 min in 4 % formaldehyde. The formaldehyde was then removed and the cells were washed three times in PBS before permeabilization in 0.2 % Triton solution for 10 min. After two successive 5-min washes in PBS, the cells were blocked in 2% BSA for 2 h. Activated caspase-3 antibody was subsequently diluted (1:500) in 1% BSA and incubated separately with the cells overnight at 4ºC. The next day, the primary antibodies were removed and the cells were washed twice before incubation for 1 h with rabbit secondary antibodies diluted (1:200) in 0.2 % BSA. Finally, the secondary antibody was removed and the cells were washed

twice in PBS before staining the nuclei with DAPI and mounting on a glass slide. Imaging and visualization were performed using the microscope Zeiss Axio.

4. Cellular uptake

Uptake of fluorescent TQ-loaded cubosomes was determined qualitatively by confocal microscopy. For confocal microscopy analysis, 70,000 cells/ml of MCF-7 cells and 60,000 cells/ml of MDA-MB-231 cells were plated on cover slips in 12-well plates, in 1 ml of respective growth medium. After treatment with Nile Red-TQ-loaded cubosomes at the indicated time points and concentrations, the cells were rinsed twice with PBS, and fixed with 4% formaldehyde solution at room temperature for 20 min. DAPI was used to stain the nuclei before mounting on glass slide. Imaging and visualization were performed using the microscope Zeiss Axio.

5. Subcellular localization

Cells were plated on cover slips in 12 well plates at a density of 70,000 cells/ml of MCF-7 cells and 60,000 cells/ml of MDA-MB-231 cells. After overnight incubation in 1 ml of respective growth medium, the medium was removed and the cells were treated for 30 min with either TQ, or blank cubosomes, or NR-TQ-loaded cubosomes. After treatment, the cells were washed twice with PBS and fixed at room temperature for 20 min in 4 % formaldehyde. The formaldehyde was then removed and the cells were washed three times in PBS before permeabilization in 0.2 % Triton solution for 10 min. After two successive 5-min washes in PBS, the cells were blocked in 2% BSA for

2 h. Caveolin, transferrin, lamp-1, and EEA-1 antibodies were subsequently diluted (1:100) in 1% BSA and incubated separately with the cells overnight at 4ºC. The next day, the primary antibodies were removed and the cells were washed twice before incubation for 1 h with mouse or rabbit secondary antibodies diluted (1:200) in 0.2 % BSA. Finally, the secondary antibody was removed and the cells were washed twice in PBS before staining the nuclei with DAPI and mounting on a glass slide. Imaging and visualization were performed using the microscope Zeiss Axio.

C. *In vivo* experiment

6-8-week-old female immunocompromised NSG mice were purchased from Biological Resource Centre. The animal protocol was approved by The NUS Institutional Animal Care and Use Committee (IACUC No. 19-04-RN547). After acclimatisation over 7 days, the mice were xenografted with human breast cancer cells (MDA-MB-231 cell line) injected subcutaneously in the right flank ($3.5*10^6$ cells resuspended in sterile physiologic NaCl solution). Once the tumor was established, the mice were divided into different treatment groups (n=6) as following:

Group 1: Vehicle control (distilled water, methanol and lipofundin), 3 days per week.

Group 2: TQ 15 mg/kg, 3 days per week.

Group 3: blank cubosomes, 3 days per week.

Group 4: TQ-loaded cubosomes, equivalent dose of TQ 15 mg/kg, 3 days per week.

TQ was dissolved in methanol and lipofundin. The tumor volume and body weight were measured 3 times per week. After 21 days of treatment, the mice were anaesthetized with inhaled isoflurane and then sacrificed by cervical dislocation and tissues were fixed in 10% neutral buffer formalin then embedded in paraffin and stored for immunohistochemistry and histological analysis. All the sections were examined by light and fluorescent microscopy.

The *in vivo* experiment was repeated twice. In the first experiment, the treatments were administered intraperitoneally. While in the second experiment, they were administered subcutaneously.

1. Hematoxylin and Eosin (H&E) staining

The samples were sectioned and stained with H&E solution. The tissue sections were examined and photographed with the microscope Olympus CX41.

2. Cellular uptake

Samples were sectioned, deparaffinized, and dehydrated, after which nuclei were stained with DAPI. Imaging and visualization were performed using the microscope Zeiss Axio.

3. Immunohistochemistry

Sections were deparaffinised, rehydrated, and subjected to antigen retrieval by microwaving in citrate buffer for 1 hour. Sections were blocked and then incubated with PCNA (Proliferating Cell Nuclear Antigen) antibody at dilutions of 1:10 overnight at 4°C. Sections were then stained with DAB working solution (Novolink™ Polymer Detection System) following manufacturer's instructions and counterstained with Haematoxylin. Tissue sections were examined and photographed with the microscope Olympus CX41.

D. Statistical analysis

All experiments (except animal studies) were performed at least three times. Data are presented as mean ± standard error (SEM). Statistical significance was set at p value 0.05. Statistical analysis was performed by t-test.

Chapter VI

Results

A. Anticancer potential of TQ-loaded cubosomes

1. TQ-loaded cubosomal nanoparticles are equally or more cytotoxic to breast cancer cell lines than free TQ and are nontoxic to nontumorigenic breast cells.

Since the activity of the prepared TQ-loaded cubosomal nanoparticles was not tested previously against cancer cell lines, we had to identify and optimize the range of active concentrations and investigate their anticancer effects. We also had to determine if the NP alone is toxic to cells and compare the active dose of the TQ- loaded cubosomes to blank NP serving as the control before testing these NPs *in vivo*. Therefore, we first tested the cytotoxic effects of the formulation *in vitro* by MTT assay (Figures 3-5). Three cell lines were used which are the nontumorigenic MCF-10A breast cells, MDA-MB-231 cancer cell line, which is an aggressive metastatic breast cancer, and MCF-7 cancer cell line which is an invasive breast ductal carcinoma cell line. The cells were treated with either free TQ, blank NP or TQ-loaded cubosomes for 24 hours.

In MCF-10A cells, TQ did not exert any toxic effects on these nontumorigenic breast cells, at concentrations ranging from 1 to 50 μM, but at higher doses there was a slight decrease in their viability. Similarly, blank NPs showed a cytotoxic effect only at concentrations higher than 30 μM. The cell viability decreased by 73% at 40 μM of blank NP. Interestingly, up to 30 μM of TQ-NP had a relatively non-cytotoxic effect on

the MCF-10A cells and cell viability was maintained at 77% at this concentration (Figure 3). Based on these experiments in non-cancerous MCF-10A breast cell line, the optimal concentrations for comparing the effects of TQ and TQ-NP was set to be below 30 μM for all future experiments.

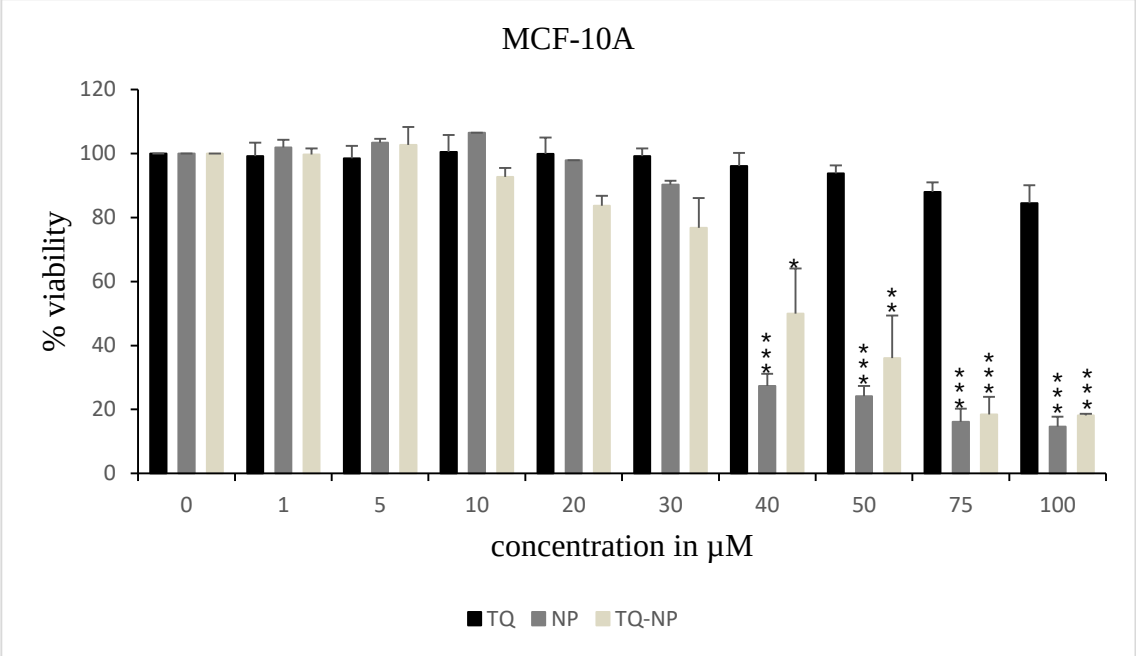

Figure 3. MTT assay showing the viability of MCF-10A cell line after 24 h of treatment with different concentrations of either TQ, or blank NP or TQ-NP (experiment was repeated three times and each experiment was done with 3 replicates per treatment, data are means ± SEM, *asterisk* indicates $p<0.05$ with respect to the control untreated cells,*$p<0.05$, **$p<0.01$, ***$p<0.001$).

At concentrations lower than 30 μM, free TQ and NP had approximately similar cytotoxic effects on MCF-7 cells. Interestingly, TQ-loaded cubosomal nanoparticles were significantly more cytotoxic than free TQ. Treatment of MCF-7 cells with TQ-NP decreased the viability of cells by 60% at 30 μM, in comparison to 30%

decrease in the presence of free TQ (Figure 4). Therefore, TQ-NP seems to form a better system of drug delivery than free TQ in this cell line.

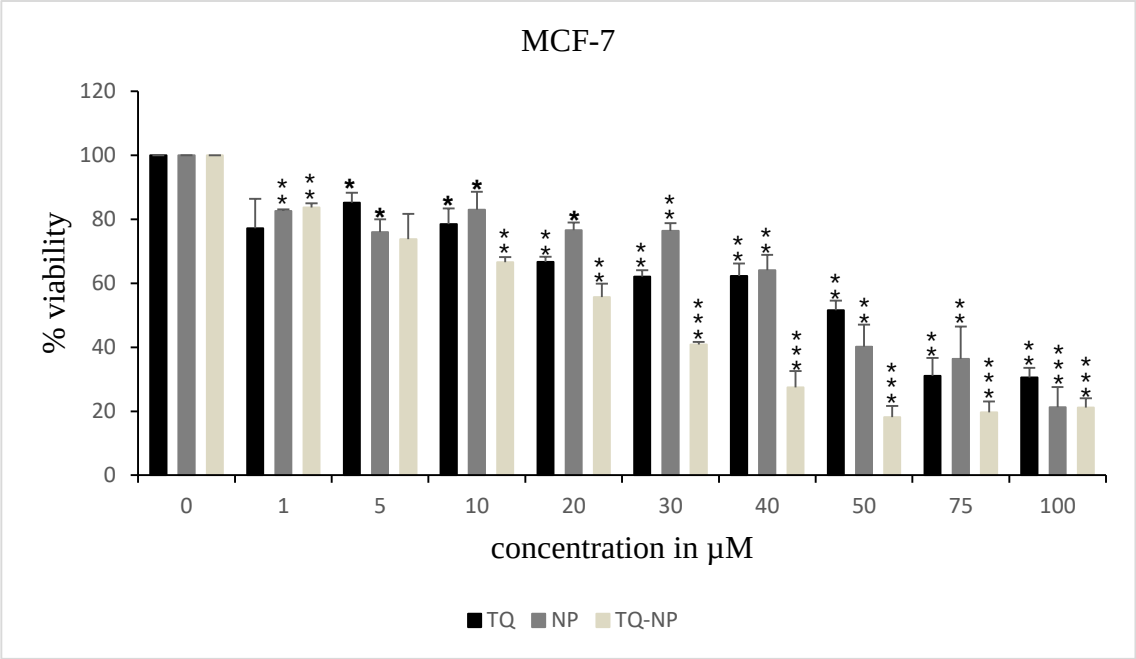

Figure 4. MTT assay showing the viability of MCF-7 cell line after 24 h of treatment with different concentrations of either TQ, or blank NP or TQ-NP (experiment was repeated three times and each experiment was done with 3 replicates per treatment, data are means ± SEM, *asterisk* indicates $p<0.05$ with respect to the control untreated cells,*$p<0.05$, **$p<0.01$, ***$p<0.001$).

Free NP had no pronounced effects on the viability of MDA-MBA-231 cells, whereby at 30 µM the viability of cells decreased by 24%. The cytotoxic effect of TQ-loaded cubosomes was more profound than free TQ; at 30 µM the cell viability in the presence of TQ was 22% in comparison to 11% with TQ-loaded cubosomes (figure 5). Thus, TQ-loaded cubosomal nanoparticles appear to form a better delivery platform than free TQ in MDA-MB-231 cells as well.

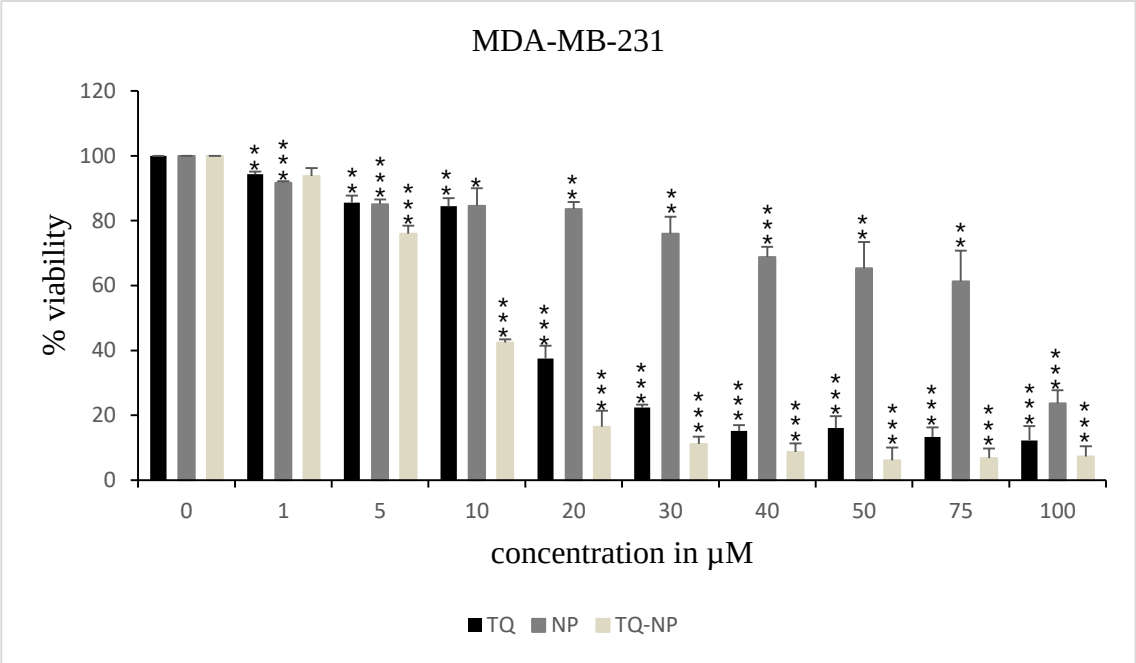

Figure 5. MTT assay showing the viability of MDA-MB-231 cell line after 24 h of treatment with different concentrations of either TQ, or blank NP or TQ-NP (experiment was repeated three times and each experiment was done with 3 replicates per treatment, data are means ± SEM, *asterisk* indicates $p<0.05$ with respect to the control untreated cells,*$p<0.05$, **$p<0.01$, ***$p<0.001$).

We also tested the cytotoxicity of the formulations on MCF-7 and MDA-MB-231 cell lines by trypan blue dye exclusion method (Figures 6-7).

When MCF-7 cells were treated with TQ-loaded cubosomes, the percentage of live cells decreased significantly at 10, 20 and 30µM (with respective percentages of 93, 86 and 63%), while the treatment with TQ significantly decreased the percentage of live cells at 10µM (0.01 p value), but the effect of TQ-NP was still more pronounced (Figure 6).

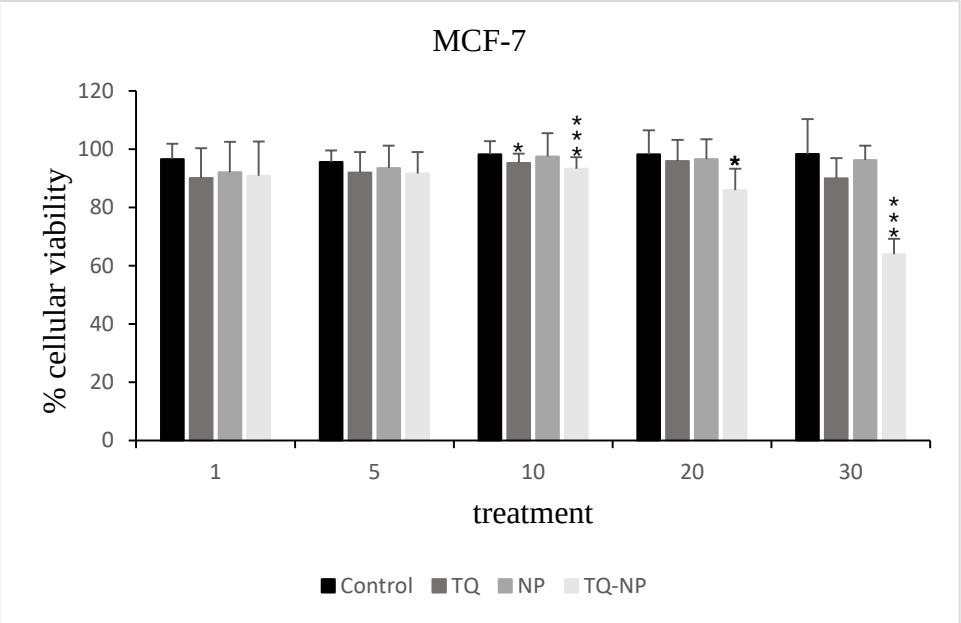

Figure 6. Trypan blue exclusion test showing the viability of MCF-7 cell line after 24 h of treatment with different concentrations of either TQ, or blank NP or TQ-NP (experiment was repeated three times and each experiment was done with duplicates per treatment, data are means ± SEM, *asterisk* indicates $p<0.05$ with respect to the untreated control,*$p<0.05$, **$p<0.01$, ***$p<0.001$).

Treatment of MDA-MB-231 cells with either TQ or TQ-loaded cubosomes caused a significant decrease in the percentage of live cells at 10, 20 and 30 µM, but the effect of TQ-loaded cubosomes was more significant than that of free TQ (Figure 7).

Therefore, a dose-dependent response was observed to treatment with TQ or TQ-loaded cubosomes in both breast cancer cell lines, whereby the viability decreased significantly as the concentration increased, and the cyctotoxic effects of TQ-loaded cubosomes was more pronounced in comparison to free TQ.

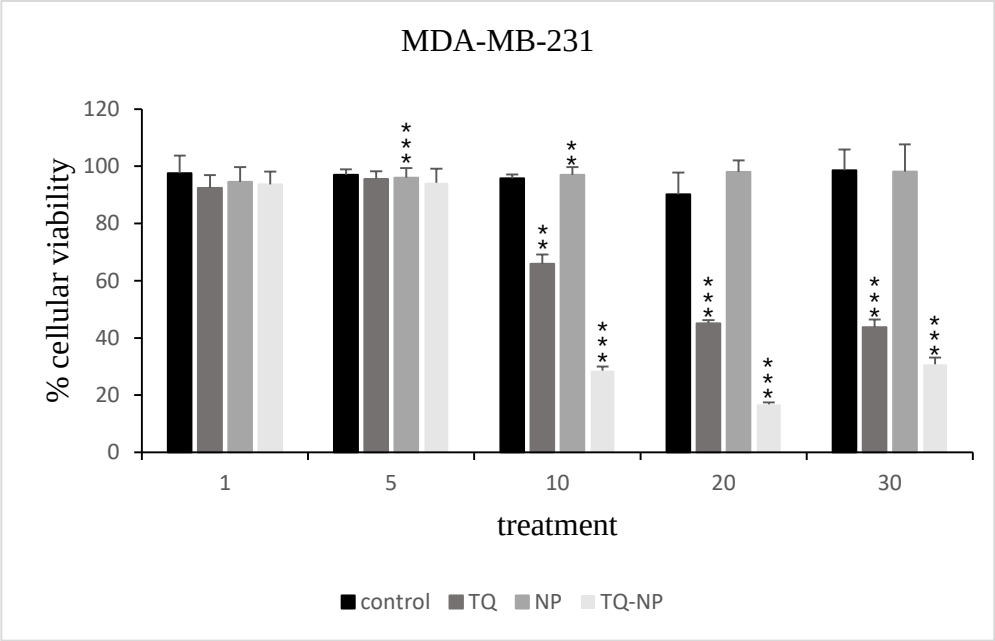

Figure 7. Trypan blue exclusion test showing the viability of MDA-MB-231 cell line after 24 h of treatment with different concentrations of either TQ, or blank NP or TQ-NP (experiment was repeated three times and each experiment was done with duplicates per treatment, data are means ± SEM, *asterisk* indicates $p<0.05$ with respect to the untreated control,*$p<0.05$, **$p<0.01$, ***$p<0.001$).

In MDA-MB-231 cell line, MTT and trypan blue exclusion assays showed approximately similar results with TQ; however, the effect of TQ-loaded cubosomes was more pronounced with MTT test in comparison to trypan blue (Table 3).

Table 3. Calculated IC_{50} values (µM) from MTT assay and trypan blue exclusion test of free TQ and TQ-loaded cubosomes in both MCF-7 and MDA-MB-231 cell lines after treatment with concentrations ranging from 1 to 100 µM and 1 to 30 µM, respectively, for 24 h.

	IC_{50} values (µM) MTT assay (1-100 µM)		IC_{50} values (µM) Trypan Blue (1-30 µM)	
Cell line	TQ	TQ-loaded cubosomes	TQ	TQ-loaded cubosomes
MCF-7	55.2	27.6	Out of range	Out of range
MDA-MB-231	27.6	7.8	22.7	14.3

2. *Free TQ and TQ-loaded cubosomes induce apoptosis in MDA-MB-231 through caspase-3 cleavage*

To assess the apoptotic effects of the compounds, we visualized the apoptotic bodies in the nuclei stained by DAPI and quantified the extent of cleavage of caspase-3 by immunohistochemistry. The number of apoptotic bodies increased in cells treated with free and encapsulated TQ (Figures 8 and 10). Active caspase-3 was significantly greater in MDA-MB-231 cells treated with free TQ and TQ-loaded cubosomes, in comparison to the untreated control. The percentage of cleaved caspase-3 in cells treated with free TQ was 71% and in those treated with TQ-loaded cubosomes was 30%. Blank cubosomes caused a non-significant change in the extent of active caspase-3 cleavage (Figure 9).

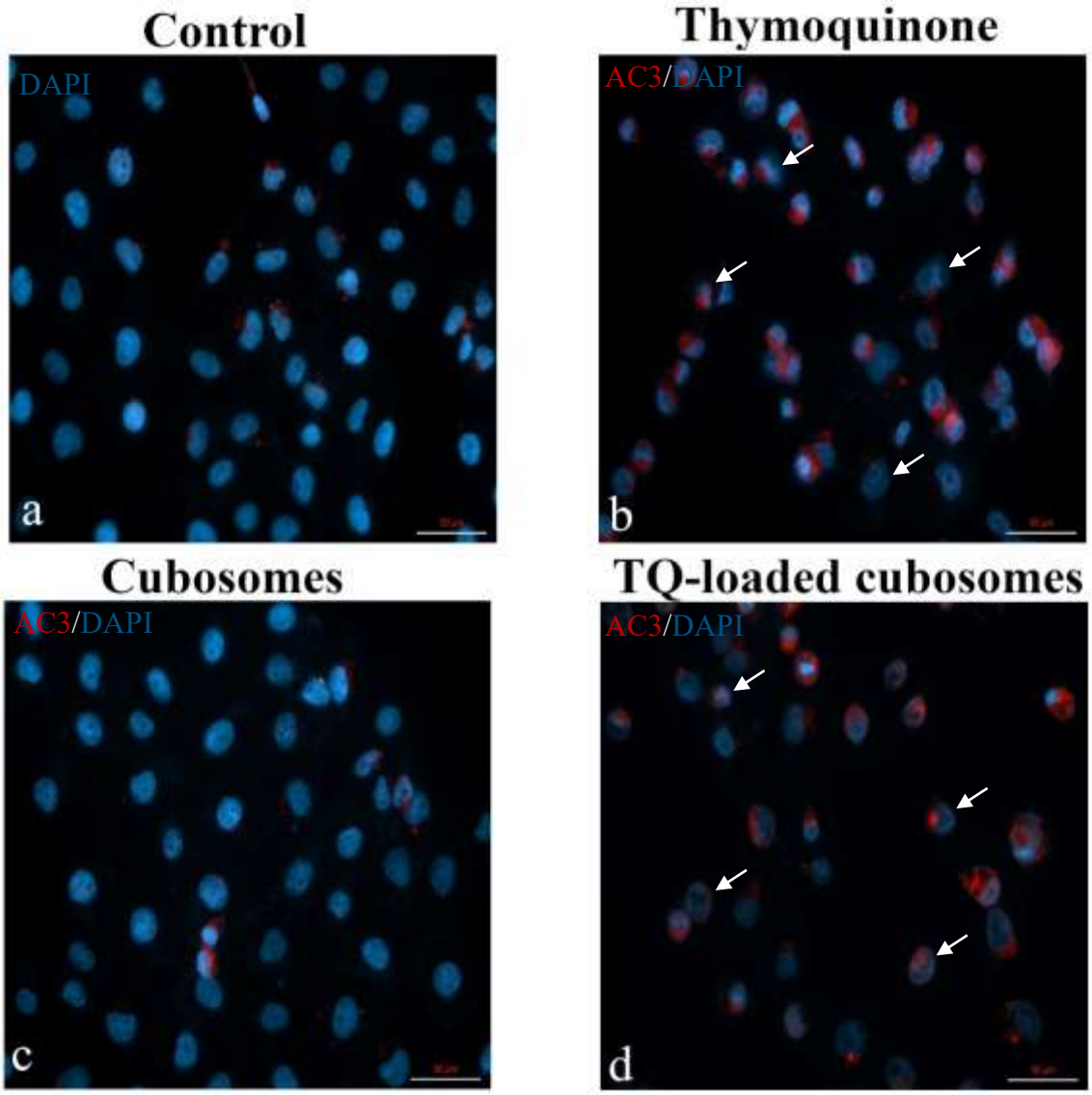

Figure 8. Immunofluorescent analysis of active caspase-3 (AC3) expression in MDA-MB-231 cell line after 24 h of treatment with TQ and TQ-loaded cubosomes using the IC_{50} values obtained from MTT assay. a) control. b) Treated with TQ (27.6 µM). c) Treated with blank cubosomes (73.4 µM). c) Treated with TQ-loaded cubosomes (7.8 µM). Arrows indicate apoptotic bodies in the nuclei stained by DAPI.
Visualized by microscope Zeiss Axio, 40X oil immersion.

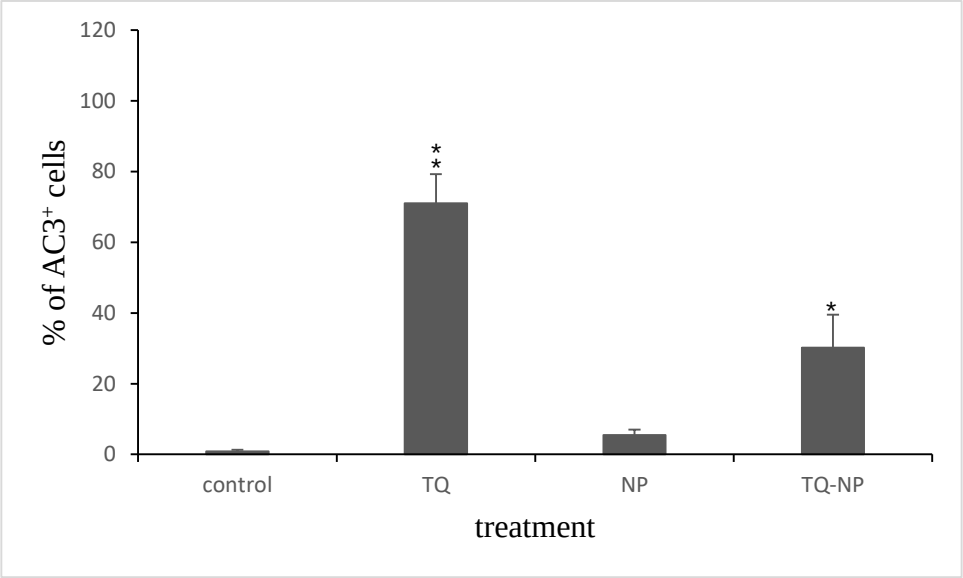

Figure 9. Active caspase-3 quantification in MDA-MB-231 cell line treated for 24 h with TQ and TQ-loaded cubosomes at the IC_{50} values obtained from MTT assay. Treatments included: free TQ (27.6 µM) or blank cubosomes (73.4 µM) or TQ-loaded cubosomes (7.8 µM). Experiment was repeated three times, data are means ± SEM, *asterisk* indicates $p<0.05$ with respect to the untreated control, *$p<0.05$, **$p<0.01$, ***$p<0.001$.Visualized by microscope Zeiss Axio, 40X oil immersion.

B. Mechanism of cellular uptake of TQ-loaded cubosomal nanoparticles

1. Internalization of TQ-loaded cubosomes by MCF-7 and MDA-MB-231 cell lines

Nile Red was coupled to cubosomes in their free and encapsulated state to track the uptake and localization of the formulations in the cells by fluorescent microscopy. After treatment of MCF-7 and MDA-MB-231 cell lines for 30 mins, the microscopic images revealed that the nanoparticles were uptaken into the cytoplasm of both breast cancer cell lines (Figures 10 and 11).

In MCF-7 cell line, blank cubosomes were evenly distributed around the nuclei of cells, while TQ-loaded cubosomes had a punctate distribution (Figure 10).

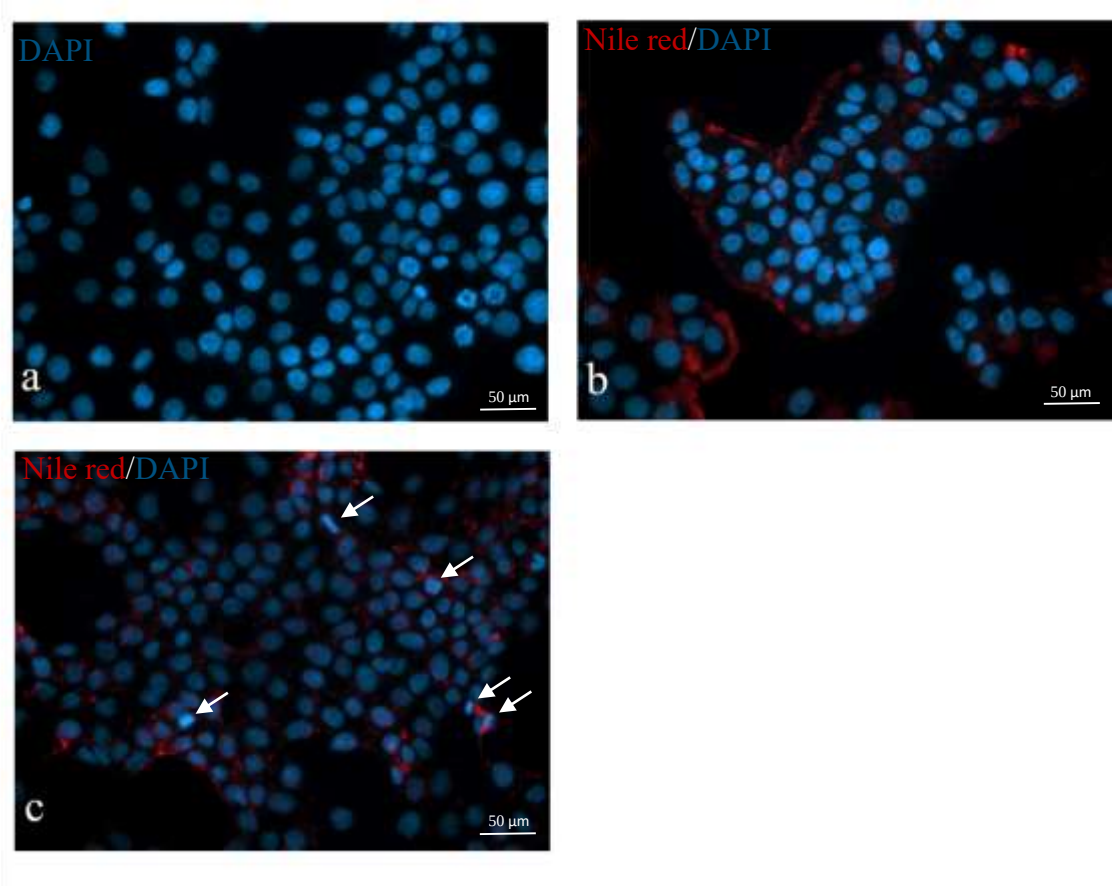

Figure 10. Cellular uptake of the formulations by MCF-7 cell line after 30 mins of treatment with the IC_{50} values obtained from MTT. a) control. b) Treated with blank cubosomes (52.5 µM). c) Treated with TQ-loaded cubosomes (27.6 µM). Arrows indicate apoptotic bodies in the nuclei stained by DAPI.
Visualized by microscope Zeiss Axio, 40X oil immersion.

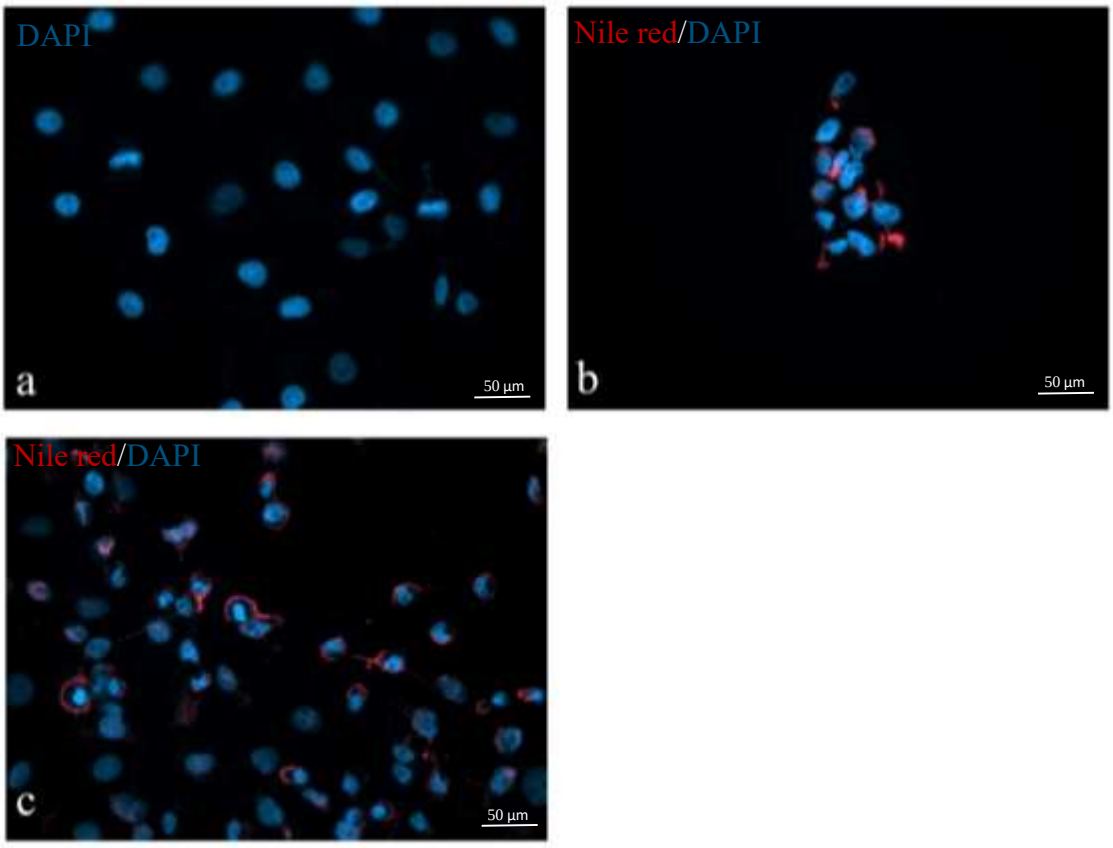

Figure 11. Cellular uptake of the formulations by MDA-MB-231 cell line after 30 mins of treatment with the IC_{50} values obtained from MTT a) control. b) Treated with blank cubosomes (73.4 µM). c) Treated with TQ-loaded cubosomes (7.8 µM). Visualized by microscope Zeiss Axio, 40X oil immersion.

2. Mechanisms of cellular uptake of cubosomes into MCF-7 and MDA-MB-231 cell lines

The cellular trafficking and localization of the formulations were investigated using the following markers: DAPI for labeling the nuclei, caveolin for labeling the caveole, LAMP for labeling the lysosomes, transferrin for identifying the clathrin coated pits and early and recycling endosomes, EEA-1 for identifying the early endosomes. Figures 12-17 show that the cubosomes, in their blank and encapsulated state, colocalize with all the markers in both cell lines, MCF-7 and MDA-MB-231. This

indicates that the cubosomes enter the cells *via* caveolin and clathrin dependent endocytosis.

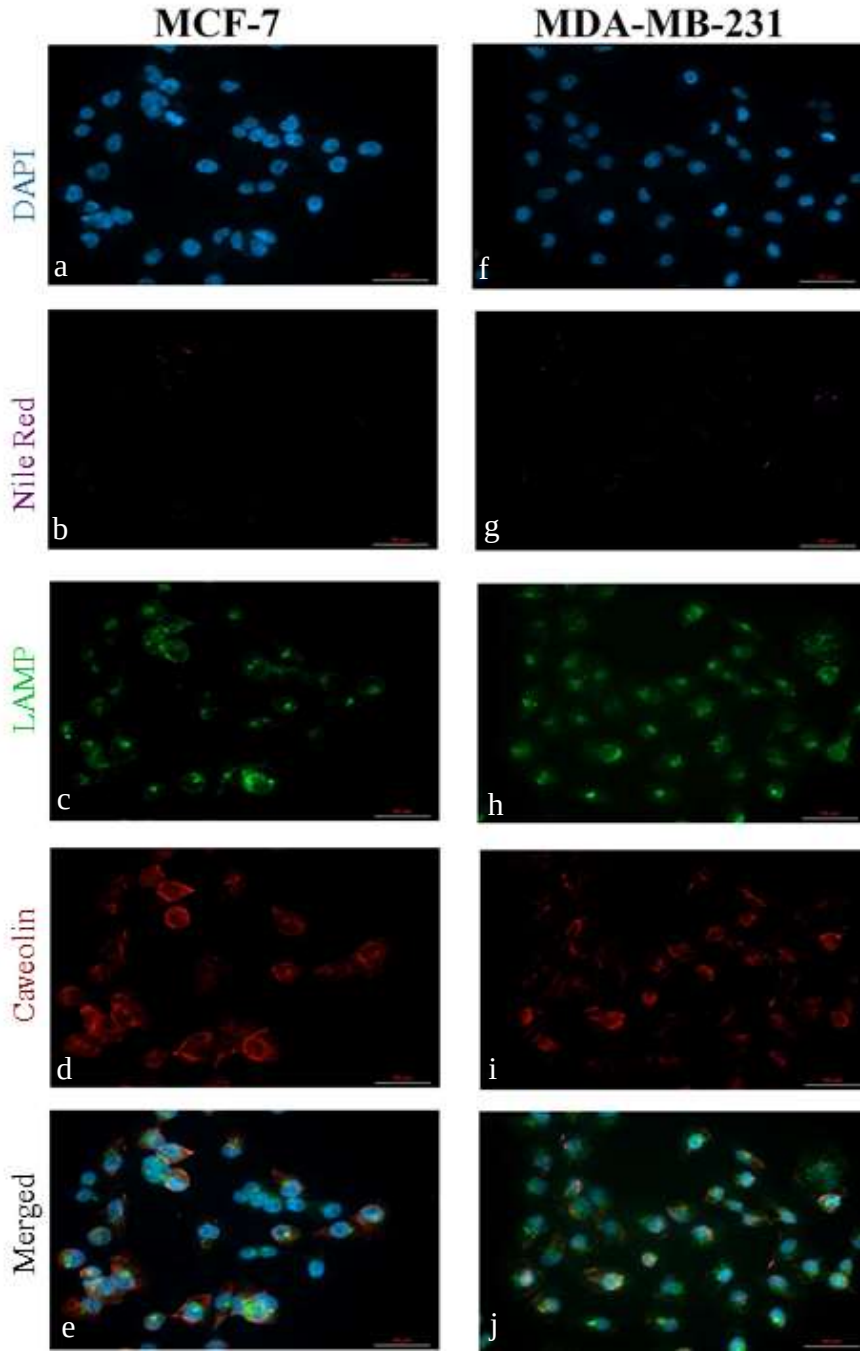

Figure 12. Immunofluorescent images of untreated cells (control), labeled with DAPI, LAMP and Caveolin. (a-e) MCF-7 cell line. (f-j) MDA-MB-231 cell line. Visualized by microscope Zeiss Axio, 40X oil immersion.

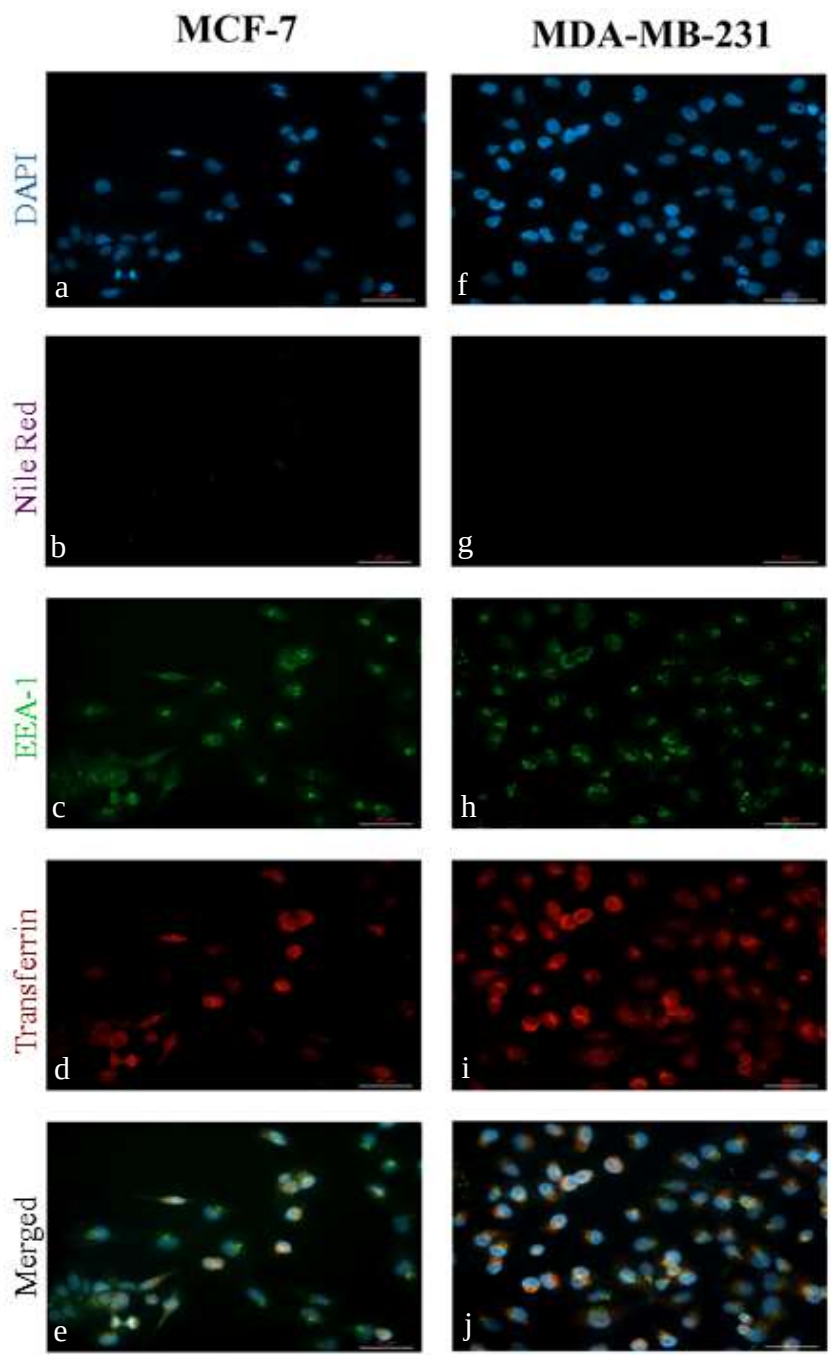

Figure 13. Immunofluorescent images of untreated cells (control), labeled with DAPI, EEA-1 and Transferrin. (a-e) MCF-7 cell line. (f-j) MDA-MB-231 cell line. Visualized by microscope Zeiss Axio, 40X oil immersion.

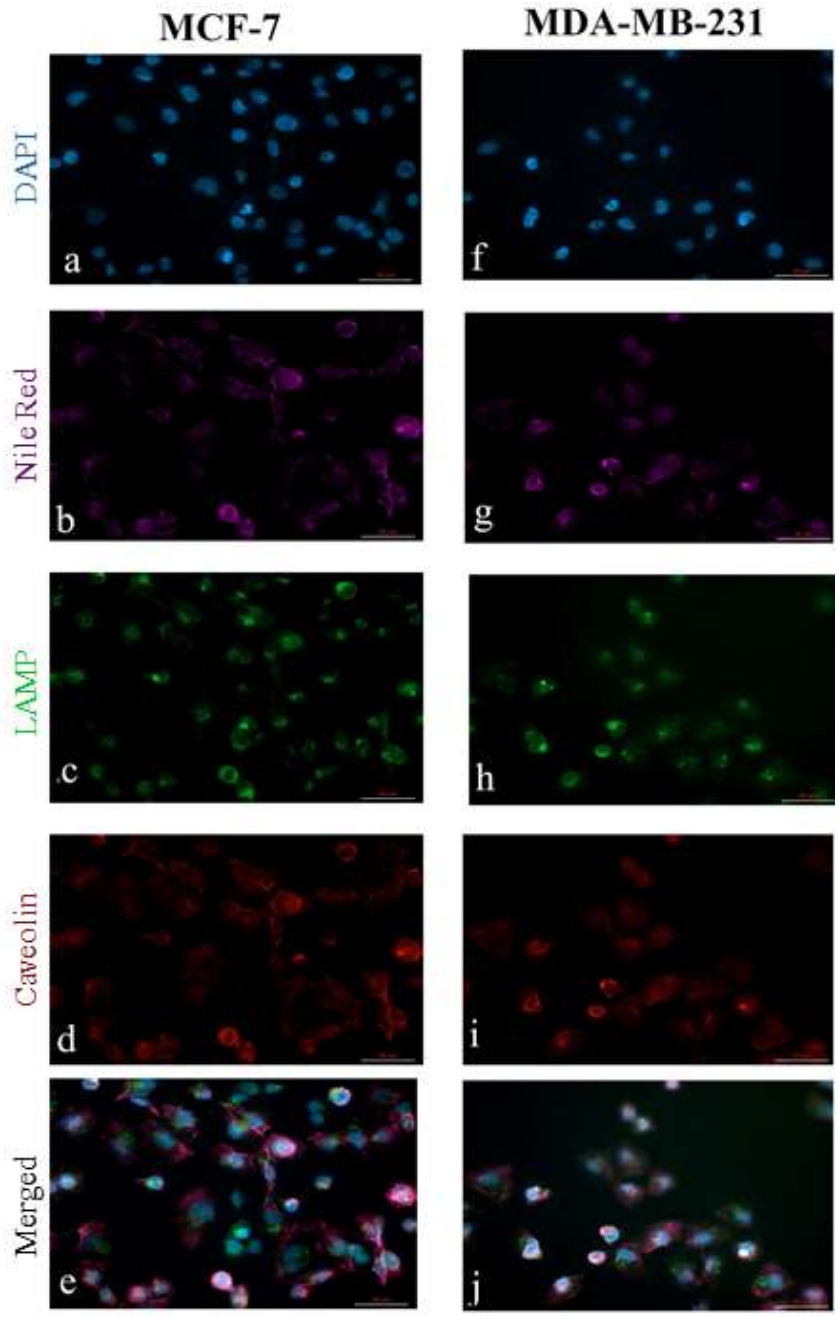

Figure 14. Subcellular localization of blank cubosomes labeled with Nile red in MCF-7 and MDA-MB-231 cell lines, treated with 52.5 µM (MCF-7) and 73.4 µM (MDA-MB-231) of blank cubosomes for 30 mins. Slides were labeled with DAPI, LAMP and Caveolin. (a-e) MCF-7 cell line. (f-j) MDA-MB-231 cell line. Visualized by microscope Zeiss Axio, 40X oil immersion.

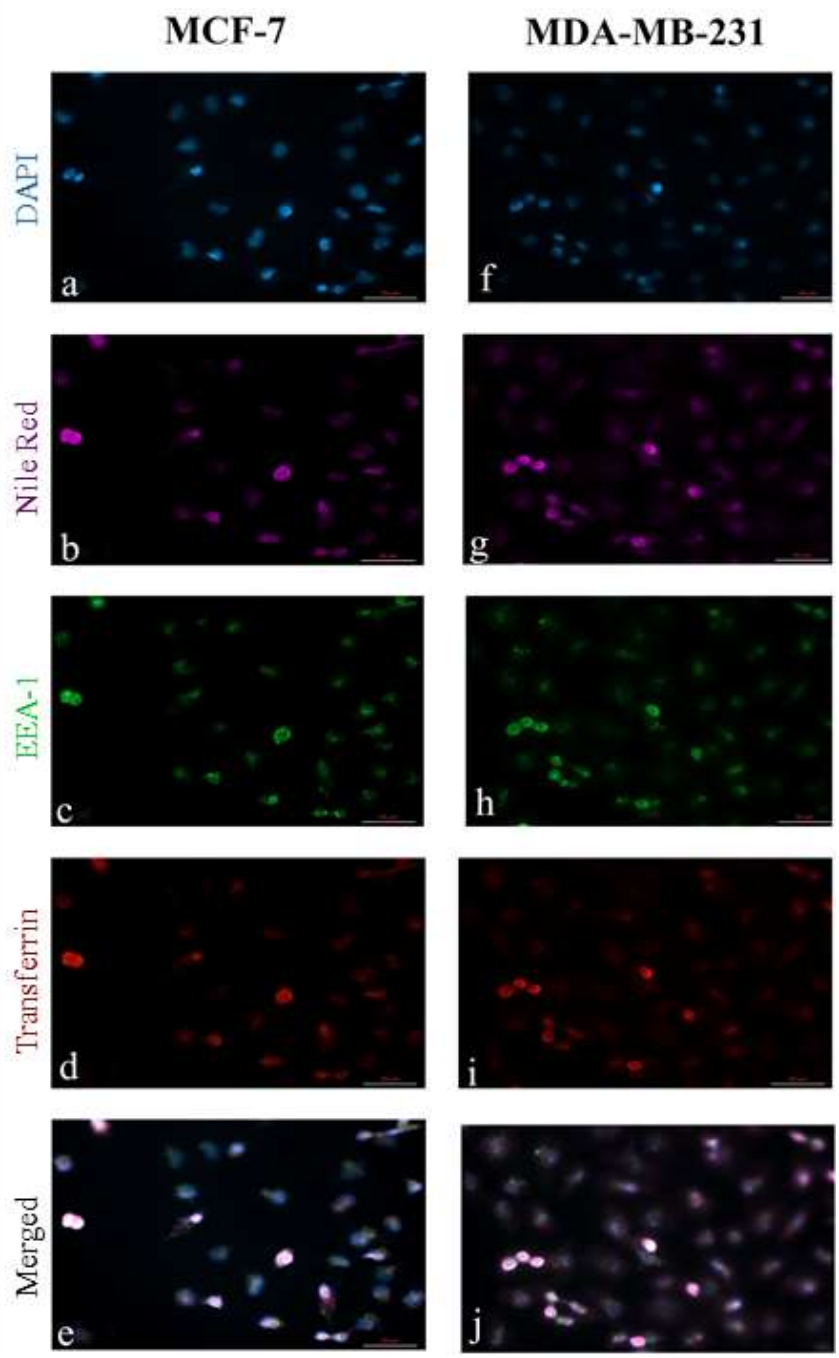

Figure 15. Subcellular localization of blank cubosomes labeled with Nile red in MCF-7 and MDA-MB-231 cell lines, treated with 52.5 µM (MCF-7) and 73.4 µM (MDA-MB-231) of blank cubosomes for 30 mins. Slides were labeled with DAPI, EEA-1 and Transferrin. (a-e) MCF-7 cell line. (f-j) MDA-MB-231 cell line. Visualized by microscope Zeiss Axio, 40X oil immersion.

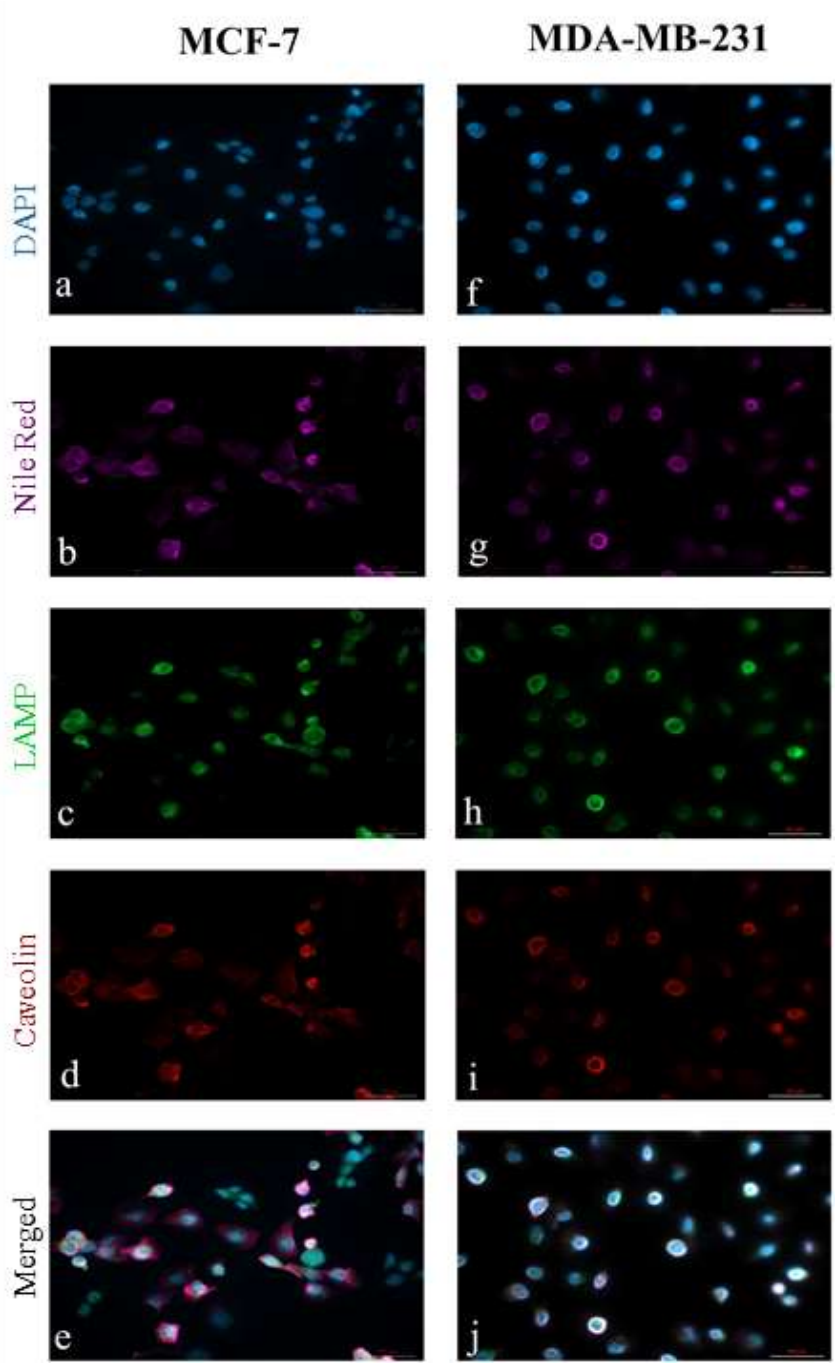

Figure 16. Subcellular localization of TQ-loaded cubosomes labeled with Nile red in MCF-7 and MDA-MB-231 cell lines. Cells were treated with 27.6 µM (MCF-7) and 7.6 µM (MDA-MB-231) of TQ-loaded cubosomes for 30 mins. Slides were labeled with DAPI, LAMP and Caveolin. (a-e) MCF-7 cell line. (f-j) MDA-MB-231 cell line. Visualized by microscope Zeiss Axio, 40X oil immersion.

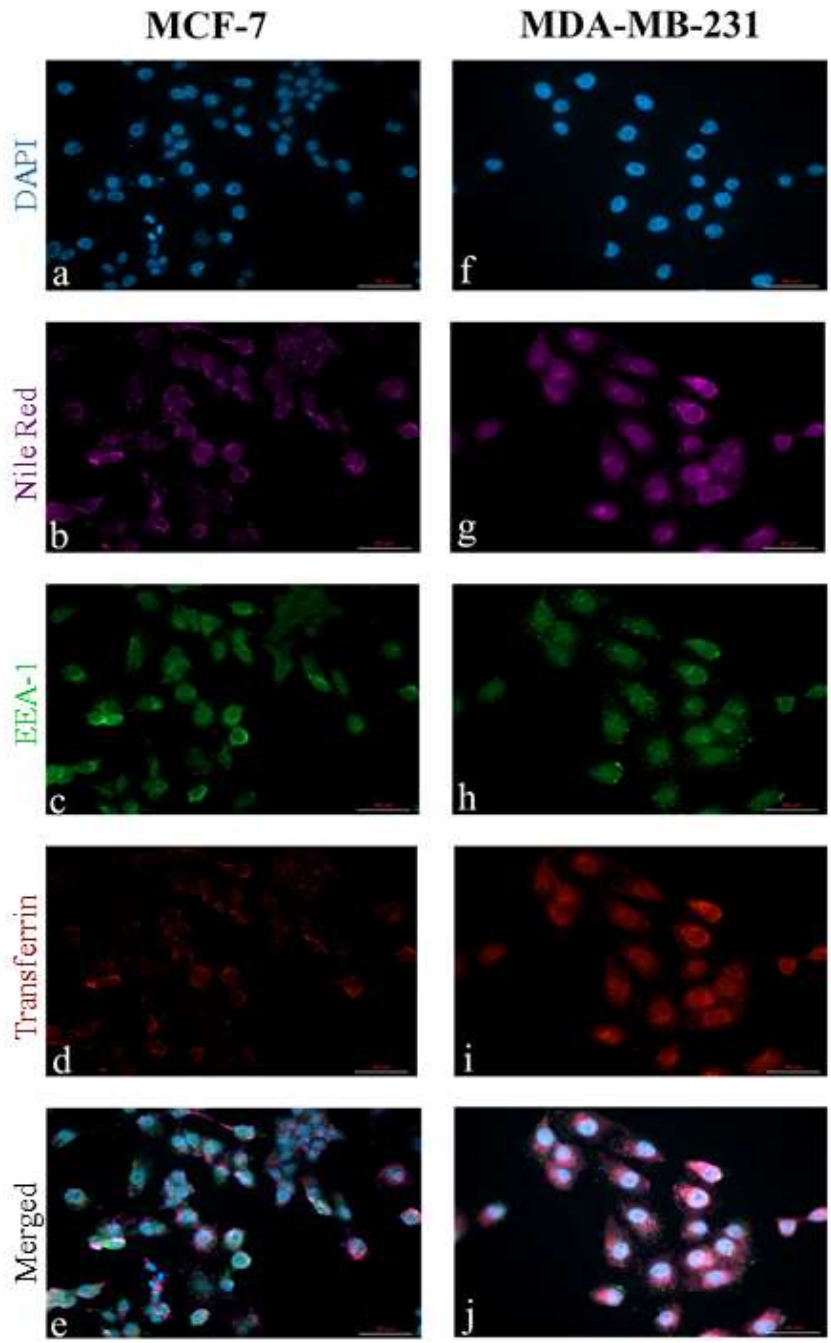

Figure 17. Subcellular localization of TQ-loaded cubosomes labeled with Nile red in MCF-7 and MDA-MB-231 cell lines, treated with 27.6 µM (MCF-7) and 7.6 µM (MDA-MB-231) of TQ-loaded cubosomes for 30 mins. Slides were labeled with DAPI, EEA-1 and Transferrin. (a-e) MCF-7 cell line. (f-j) MDA-MB-231 cell line. Visualized by microscope Zeiss Axio, 40X oil immersion.

C. Anticancer activity of intraperitoneally administered TQ-loaded cubosomes in breast cancer xenograft models

To assess the activity of the TQ-loaded cubosomes in animal models and to determine whether the formulation confers an advantage over free TQ, 6 to 8-week-old female immunocompromised NSG mice were used.

A pilot study using four NSG mice was performed to confirm tumor development after subcutaneous injection of $3.5*10^6$ MDA-MB-231 human breast cancer cells in the right flank. Tumors appeared after 7 days of injection.

In the first *in vivo* experiment, where the treatments were injected intraperitoneally after tumor development, mice treated with TQ showed a significant decrease in the tumor volume with a rapid decrease in body weight which led to the death of one of the mice at the 7^{th} day of treatment, in comparison to the control group that showed a normal steady increase in the tumor volume and a slight non-significant change in body weight (Figures 18 and19). Those treated with TQ were hyperactive and aggressive.

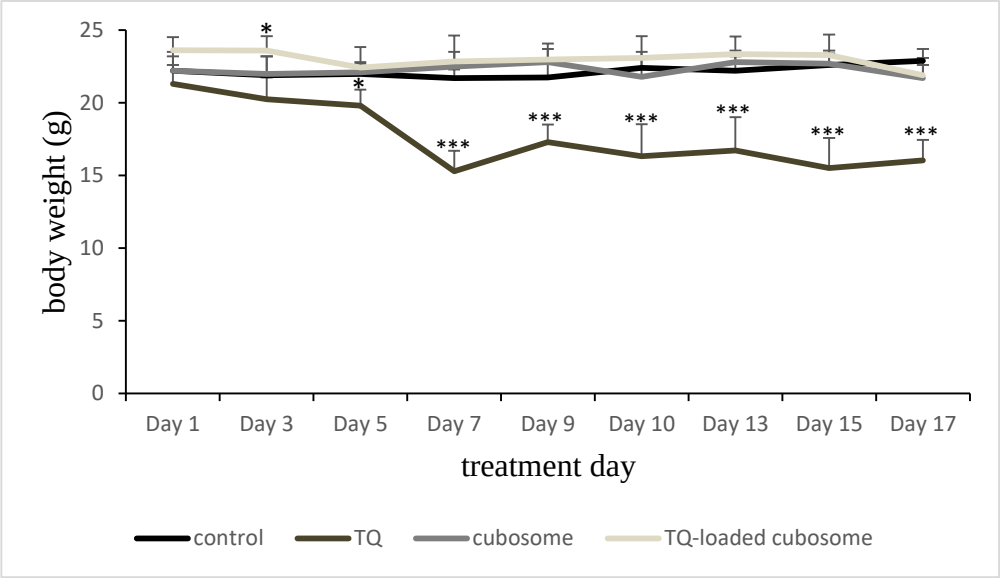

Figure 18. Graph showing the variation in the body weight of the 4 groups of mice (measured 3 times/week) as a function of time (days). Treatment was given intraperitoneally. Data are means ± SD, *asterisk* indicates $p<0.05$ with respect to the control, *$p<0.05$, **$p<0.01$, ***$p<0.001$

Mice treated with blank cubosomes showed an increase in the volume of tumors in comparison to the control group with a slight non-significant change in body weight (Figures 18 and19).

Mice treated with TQ-loaded cubosomes showed an increase in tumor volume which was less pronounced than those treated with blank NP and greater than the control group, with significant differences at days 9 and 15 and non-significant change in body weight (Figures 18 and19). Mice treated with blank cubosomes and TQ- loaded cubosomes showed fluid retention in the abdomenal region and were aggressive and distressed (Figure 20).

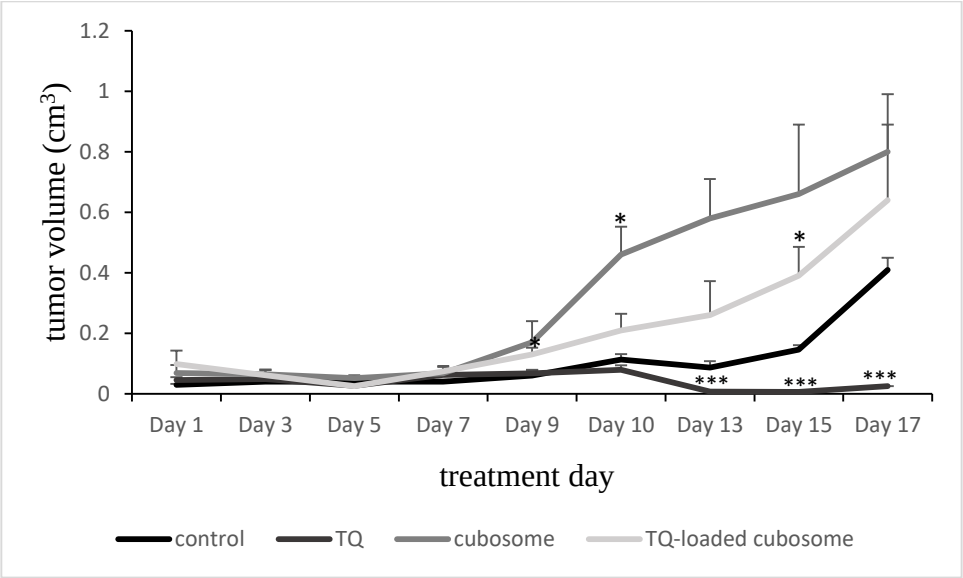

Figure 19. Graph showing the variation in the tumor volume of the 4 groups of mice (measured by vernier caliper, 3 times/week) as a function of time (days). Treatment was given intraperitoneally. Data are means ± SEM, *asterisk* indicates $p<0.05$ with respect to the control, *$p<0.05$, **$p<0.01$, ***$p<0.001$

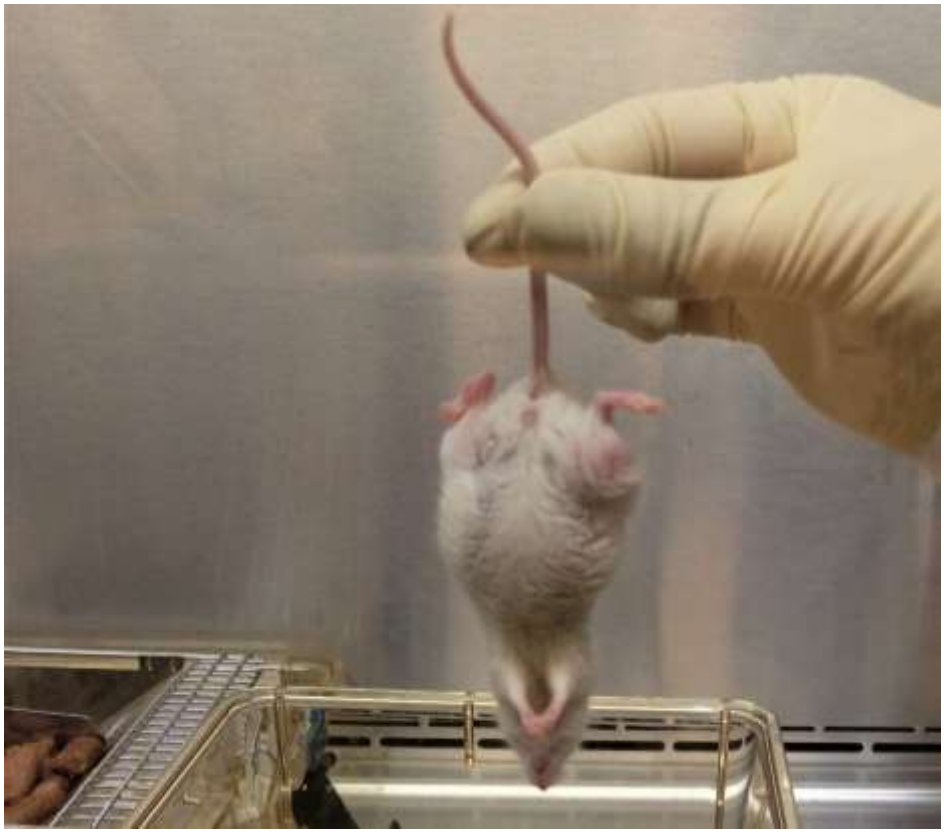

Figure 20. Mouse treated with blank cubosomes showing fluid retention in the area of intraperitoneal injection.

Control **Thymoquinone** **Cubosomes** **TQ-loaded Cubosomes**

Figure 21. Mice at day 21, day of sacrifice, after treating them intraperitoneally with either the vehicle, or blank cubosome, or 15 mg/kg TQ or its equivalent in TQ-loaded cubosomes.

1. Hematoxylin and Eosin staining of tumor tissues

H&E staining of the tumor tissues from mice treated intraperitoneally showed a difference in the tissue architecture and organization. The number of nuclei differed among the mice groups, such that the mice treated with TQ-loaded cubosomes had the fewest nuclei, in comparison to all other groups (Figure 22).

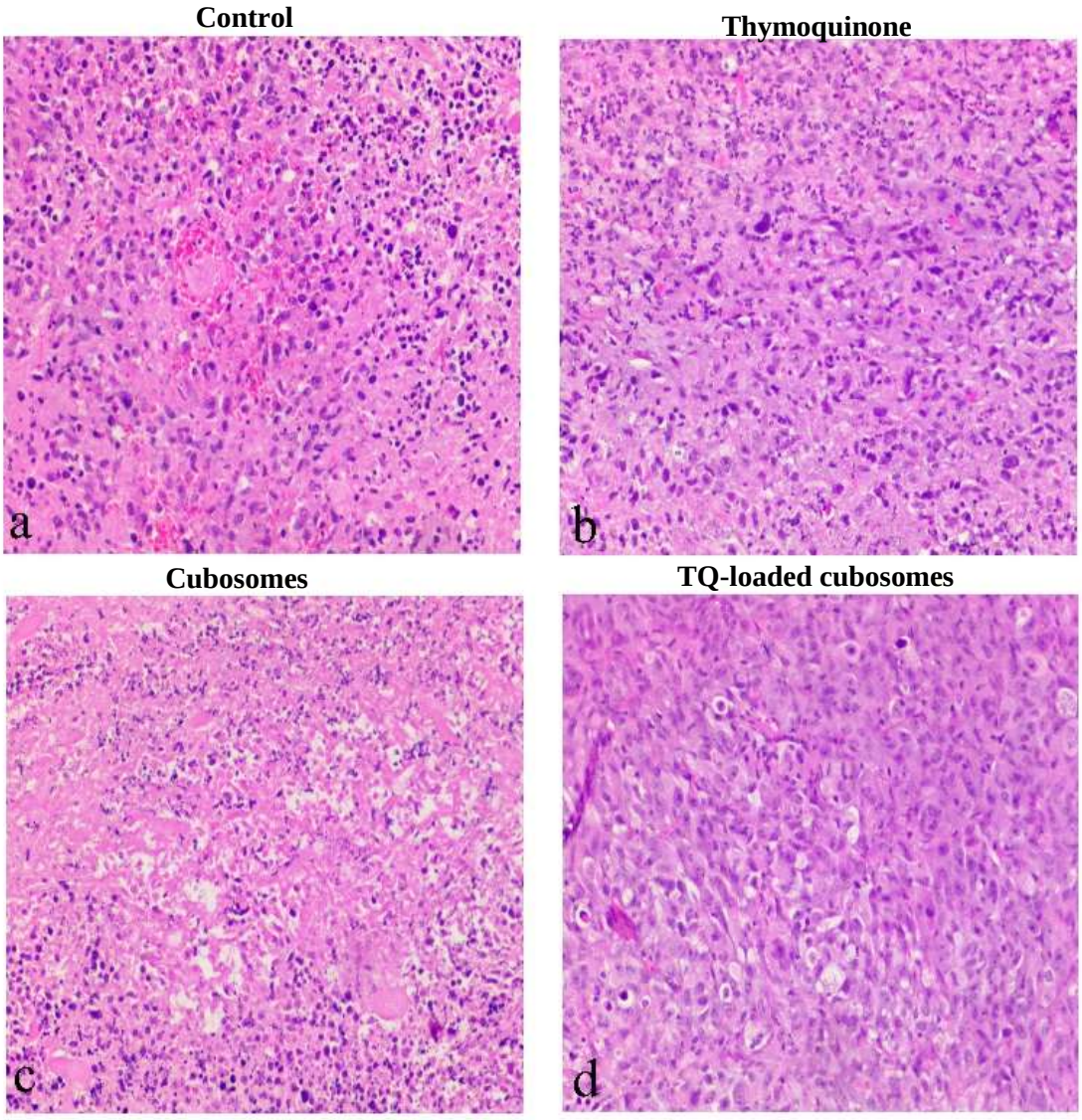

Figure 22. Hematoxylin and Eosin (H&E) staining of tumor tissues from mice treated intraperitoneally with either a) vehicle. b) 15 mg/kg TQ. c) blank cubosomes. d) its equivalence in TQ-loaded cubosomes. Visualized by the microscope Olympus CX41, 100X magnification.

2. Cellular uptake of the cubosomal nanoparticles in mice (experiment 1)

To determine the cellular uptake of the nanoparticles, the nuclei were stained with DAPI and the nanoparticles were conjugated to the Nile Red dye. However, the fluorescent microscopic images of the kidney, liver and tumor slides did not show any signal (Figure 23).

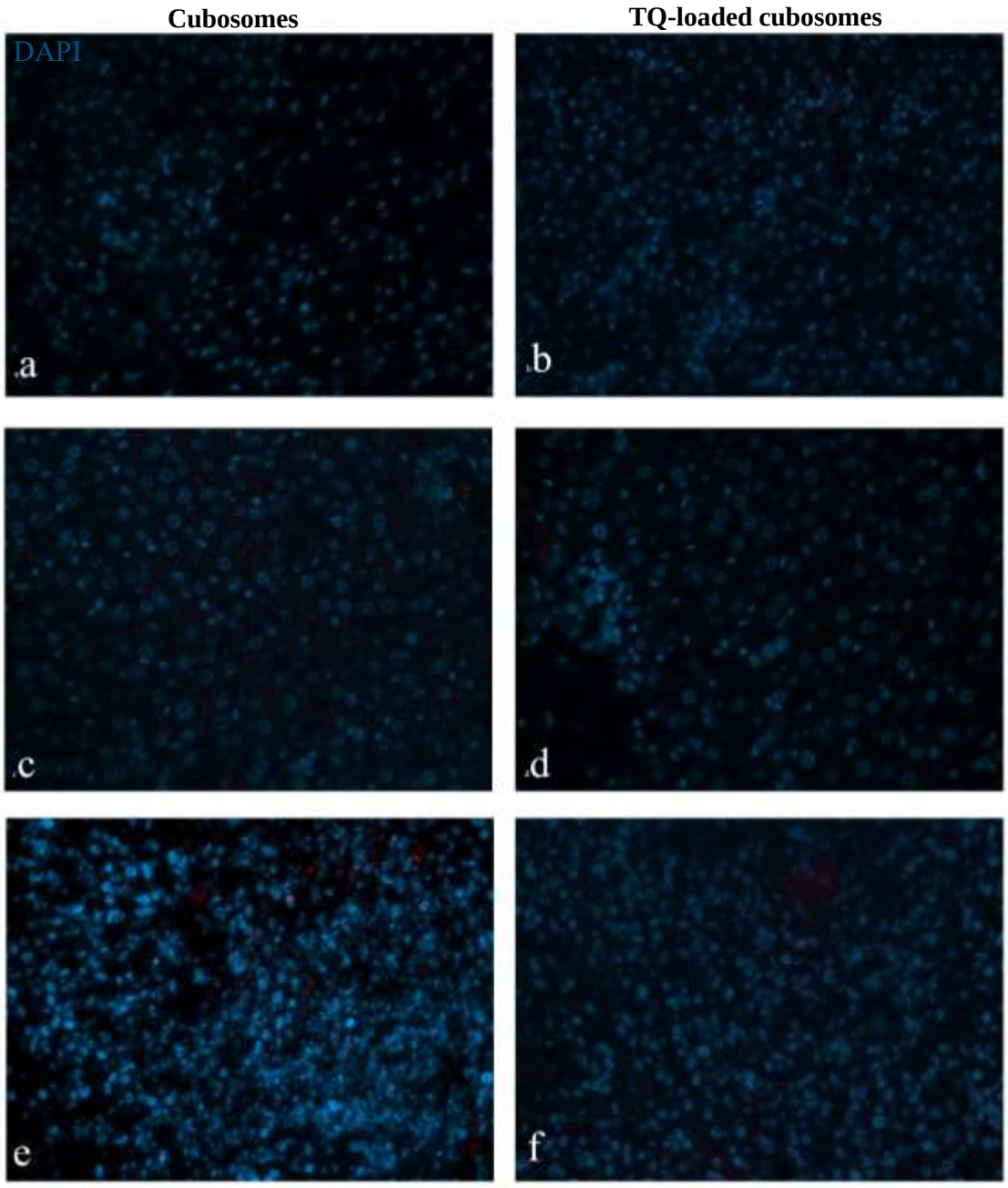

Figure 23. Cellular uptake of cubosomes and TQ-loaded cubsosmes into cells in mice treated intraperitoneally. a) kidney, cubosome. b) kidney, TQ-loaded cubosomes. c) liver, cubosome. d) liver, TQ-loaded cubosomes. e) tumor, cubosome. f) tumor, TQ-loaded cubosomes. Visualized by microscope Zeiss Axio, 40X oil immersion.

3. PCNA expression in mouse tumors by immunohistochemistry

In the first *in vivo* experiment, immunohistochemistry analysis of PCNA expression in the following tissues, -kidney, liver and tumor-, showed that there is significant decrease in PCNA expression in the tumor tissues in mice treated with blank cubosomes and TQ-loaded cubosomes ($p<0.001$ and $p<0.01$, respectively). PCNA expression decreased significantly in the kidney tissue in mice treated with TQ-loaded cubosomes, while no significant change was shown in the remaining tissues (Figure 25).

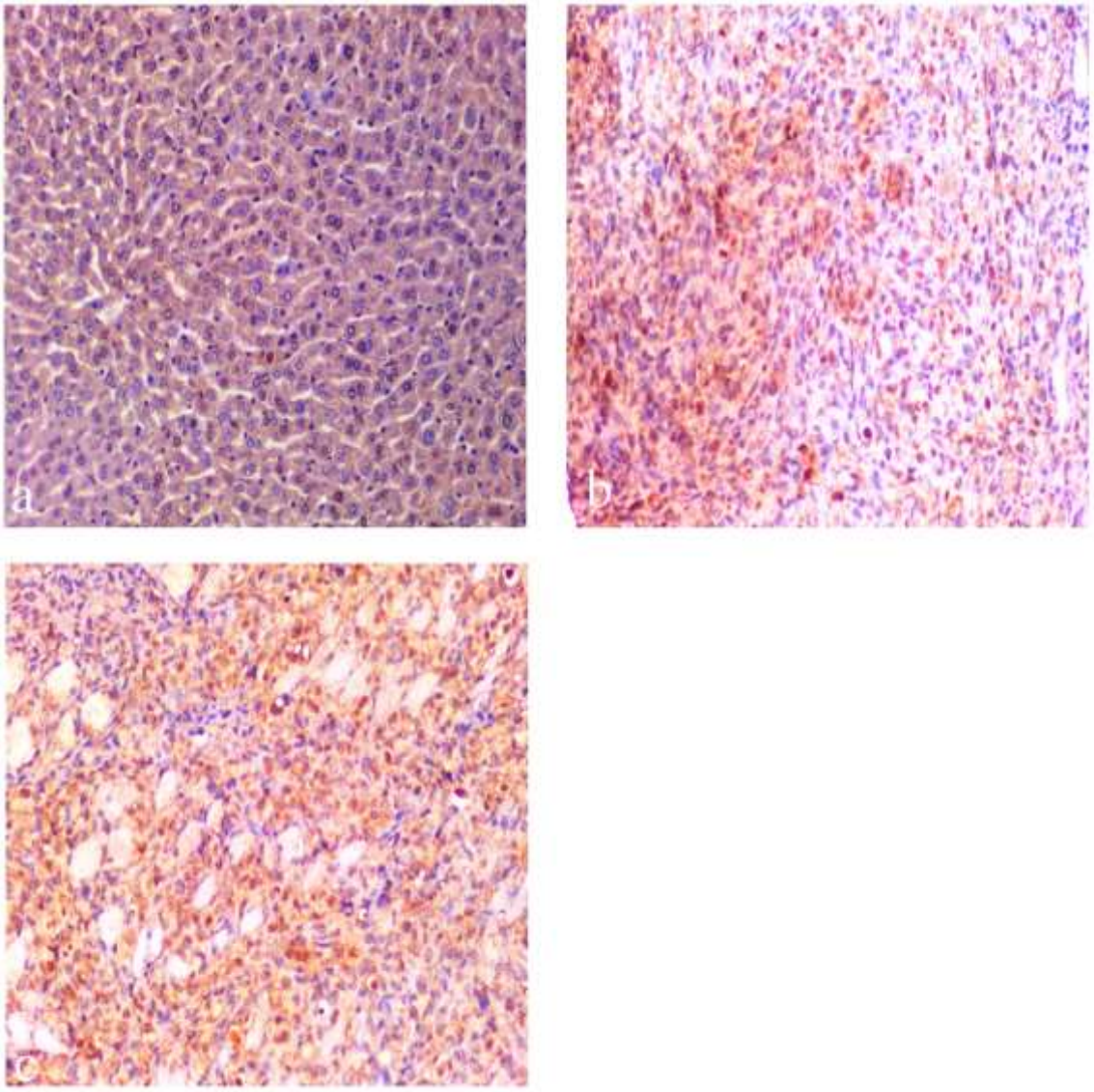

Figure 24. Immunohistochemistry analysis of PCNA expresssion in tumor tissues from mice treated intraperitoneally with either a) vehicle. b) blank cubosomes. c) TQ-loaded cubosomes. Visualized by the microscope Olympus CX41, 100X magnification.

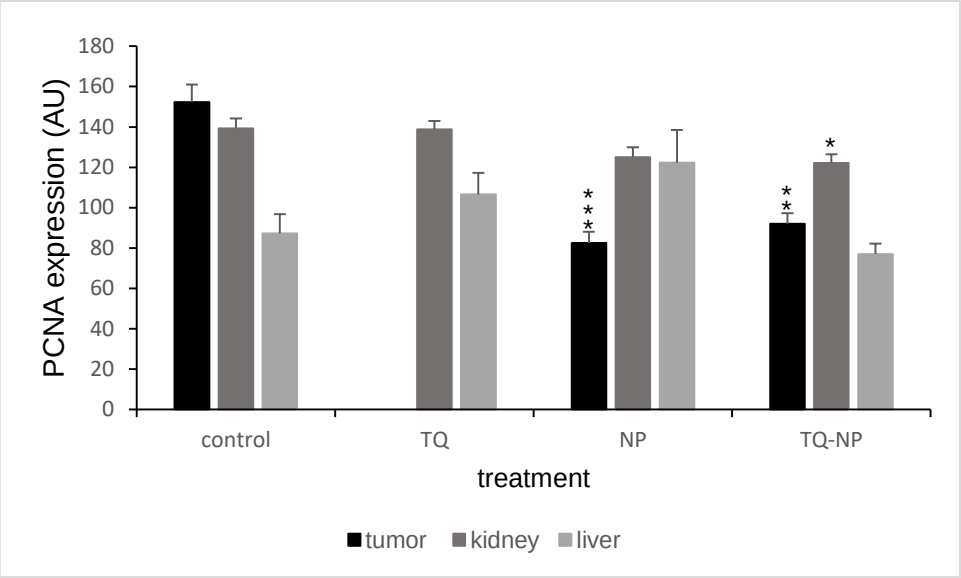

Figure 25. PCNA expression (AU) in kidney, liver and tumor from mice treated intraperitoneally with either the vehicle, or 15 mg/kg TQ, or its equivalent in TQ-loaded cubosomes, or blank cubosomes. Data are means ± SEM, *asterisk* indicates $p<0.05$ with respect to the control, *$p<0.05$, **$p<0.01$, ***$p<0.001$.

D. Anticancer activity of subcutaneously administered TQ-loaded cubosomes in breast cancer xenograft models

The *in vivo* experiment was repeated. The same treatment protocol was followed, but the treatments were injected subcutaneously to reduce the side effects.

In the second *in vivo* experiment, mice in all groups showed a slight non-significant increase in both their body weights and tumor volumes. No side effects were reported in any group (Figure 26 amd 27).

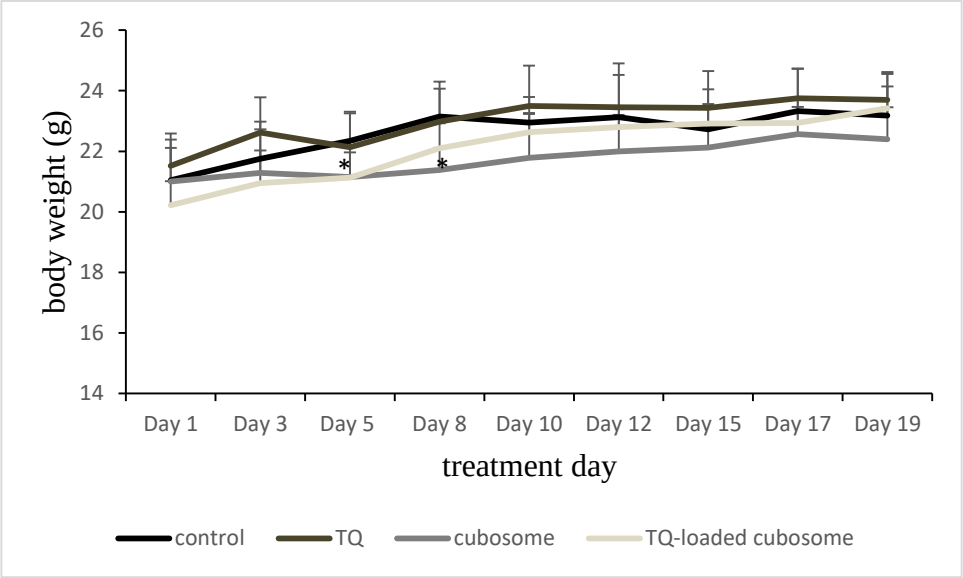

Figure 26. Graph showing the variation of the body weight of the 4 groups of mice (measured 3 times/week) as a function of time (days), treated subcutaneously. Data are means ± SD, *asterisk* indicates p<0.05 with respect to the control, *p<0.05, **p<0.01, ***p<0.001.

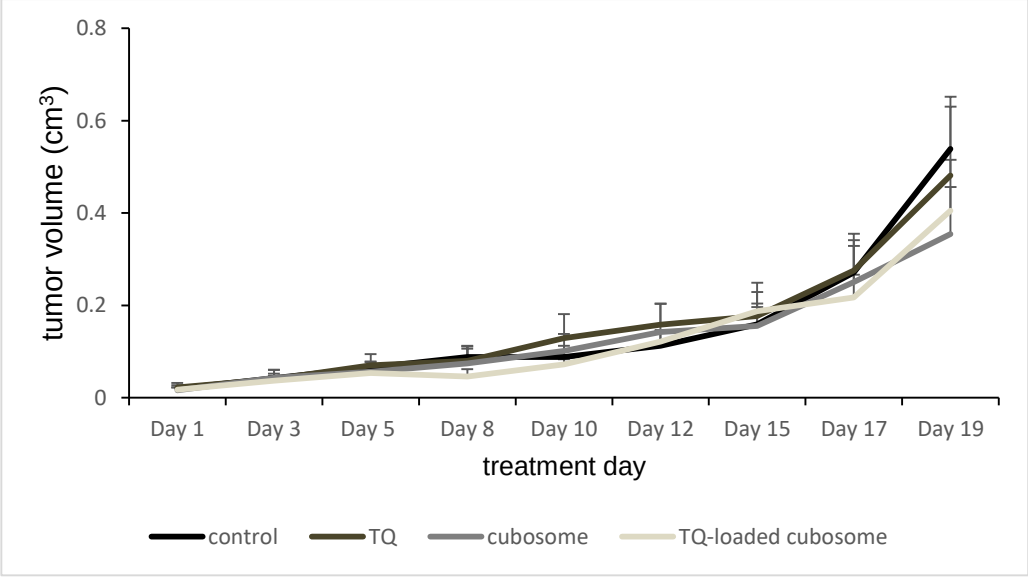

Figure 27. Graph showing the variation of the tumor volume of the 4 groups of mice (measured by vernier caliper, 3 times/week) as a function of time (days), treated subcutaneously. Data are means ± SEM, *asterisk* indicates p<0.05 with respect to the control, *p<0.05, **p<0.01, ***p<0.001.

Control **Thymoquinone** **Cubosomes** **TQ-loaded Cubosomes**

Figure 28. Mice at day 21, day of sacrifice, after treating them subcutaneously with either the vehicle, or blank cubosome, or 15 mg/kg TQ or its equivalent in TQ-loaded cubosomes.

1. Hematoxylin and Eosin staining of tumor tissues

H&E staining of the tumor tissues from the mice that were treated subcutaneously did not show a pronounce difference in the tissue architecture and organization. The number of nuclei is approximately the same in all mice groups (Figure 29).

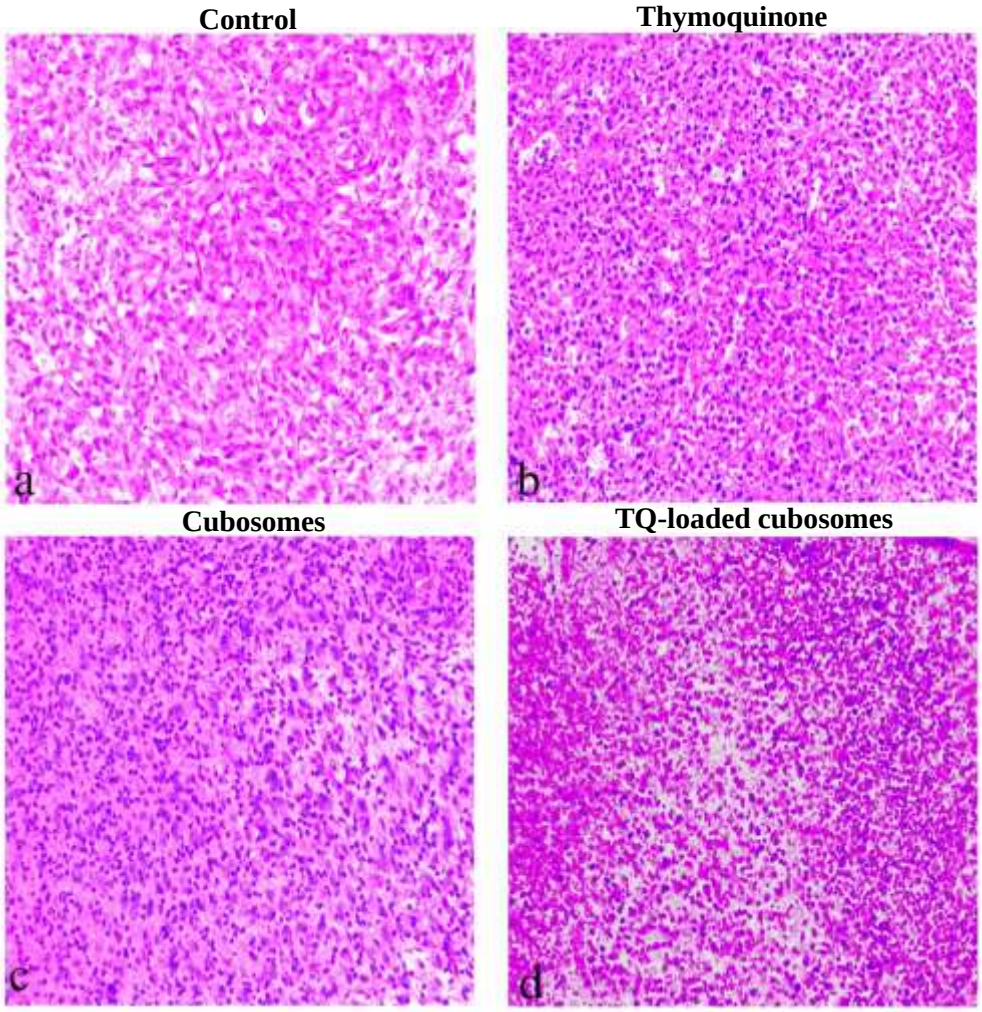

Figure 29. Hematoxylin and Eosin (H&E) staining of tumor tissues from mice treated subcutaneously with either a) vehicle. b) 15 mg/kg TQ. c) blank cubosomes. d) its equivalence in TQ-loaded cubosomes. Visualized by the microscope Olympus CX41, 100X magnification.

2. Cellular uptake of the cubosomal nanoparticles in mice (experiment 2)

Similarly, in the second *in vivo* experiment, there was no uptake of the cubosomes and TQ-loaded cubosomes coupled to Nile Red dye, except in one image which is the tumor tissue from mice treated with blank cubosomes (Figure 30).

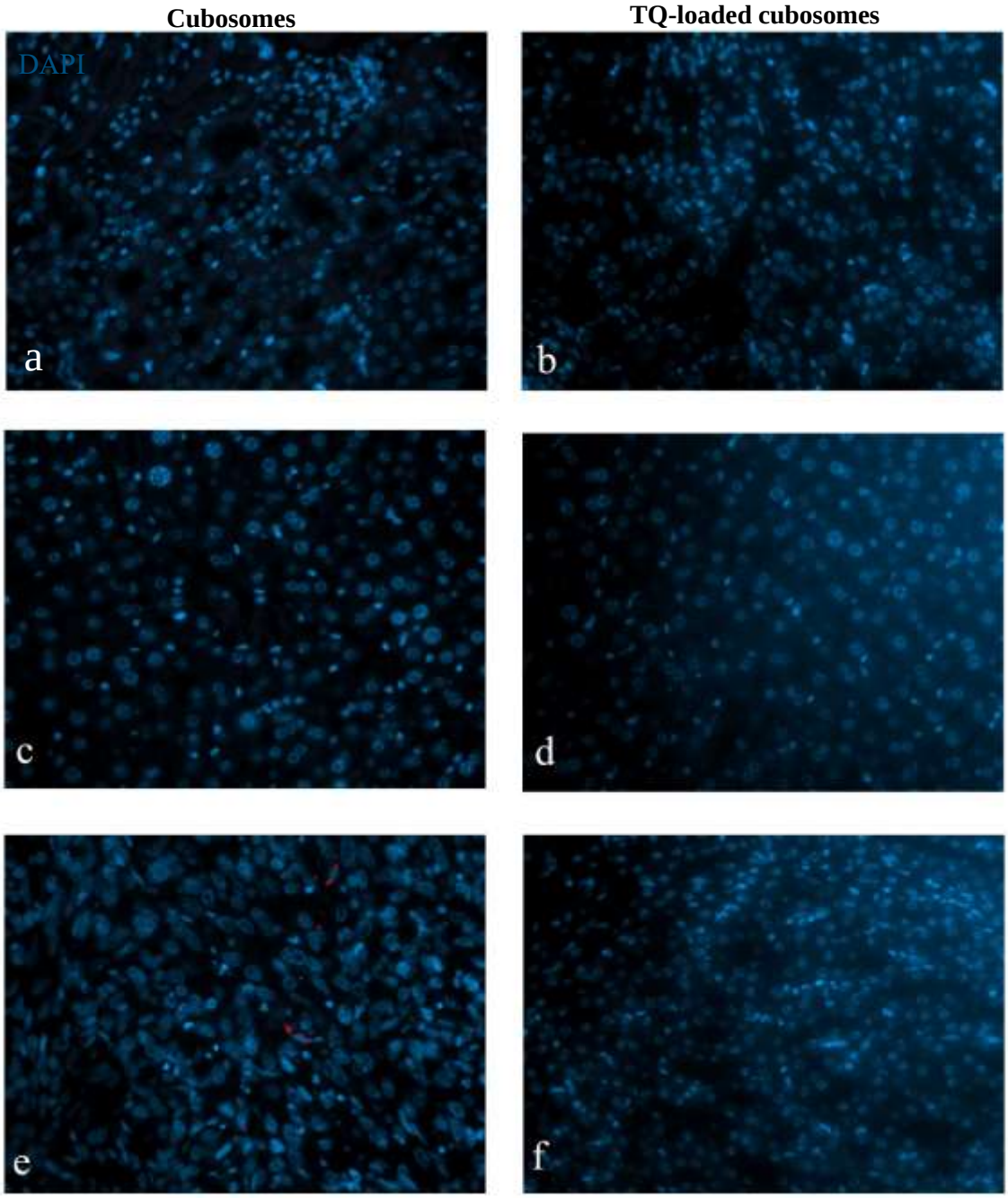

Figure 30. Cellular uptake of cubosomes and TQ-loaded cubosomes into the cells in mice treated subcutaneously. a) kidney, cubosome. b) kidney, TQ-loaded cubosomes. c) liver, cubosome. d) liver, TQ-loaded cubosomes. e) tumor, cubosome. f) tumor, TQ-loaded cubosomes. Visualized by microscope Zeiss Axio, 40X oil immersion.

3. PCNA expression by immunohistochemistry

In the second *in vivo* experiment, there was non-significant change in the PCNA expression in the tumor tissues in all mice groups. While it significantly increased and decreased in mice treated with blank cubosomes and TQ-loaded cubosomes in the kidney and liver tissues, repectively (Figure 32).

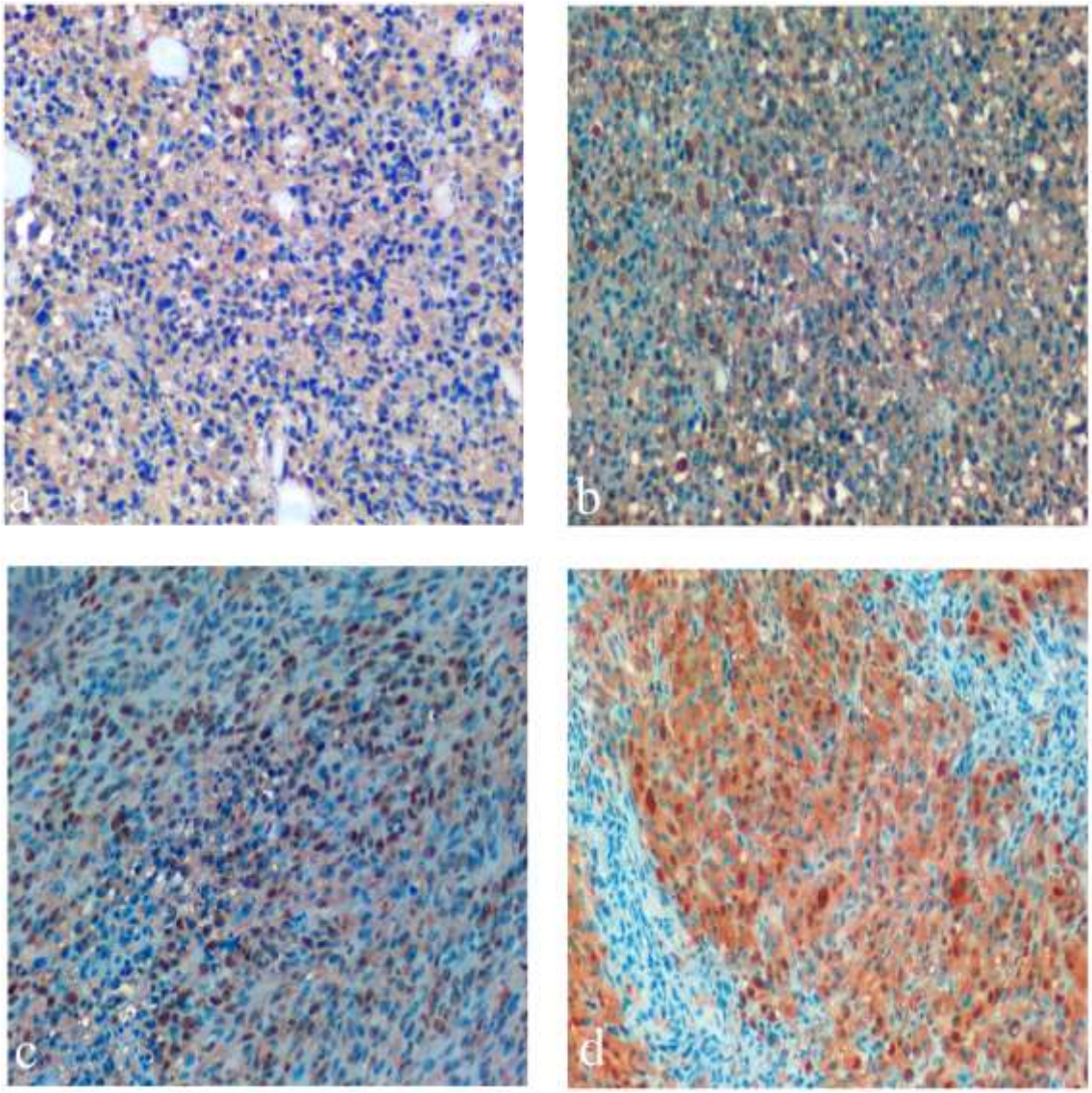

Figure 31. Immunohistochemistry analysis of PCNA expresssion in tumor tissues from mice treated subcutaneously with either a) vehicle. b) 15 mg/kg TQ. c) blank

cubosomes. d) TQ-loaded cubosomes. Visualized by the microscope Olympus CX41, 100X magnification.

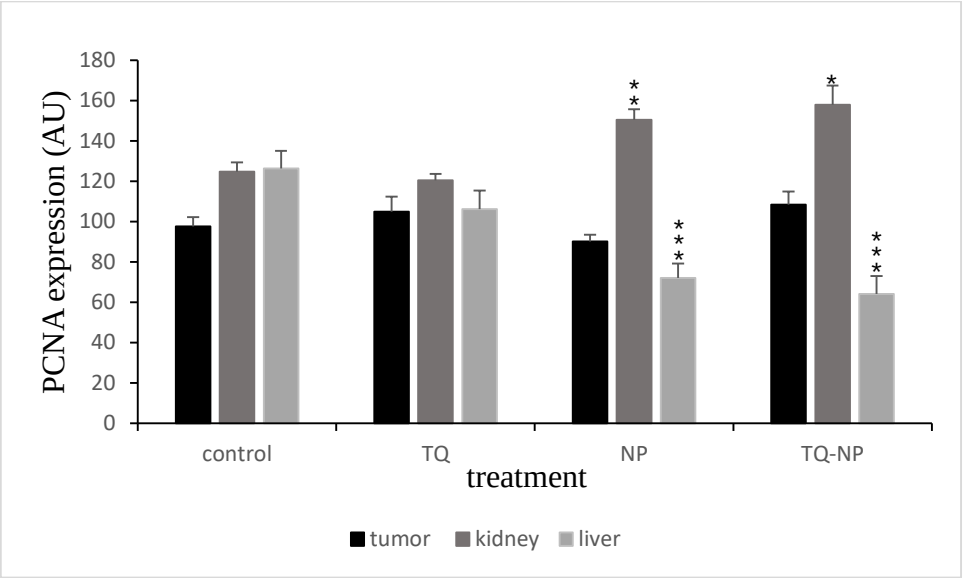

Figure 32. PCNA expression (AU) in kidney, liver and tumors derived from mice treated subcutaneously with either the vehicle, or 15 mg/kg TQ, or its equivalent in TQ-loaded cubosomes, or blank cubosomes. Data are means ± SEM, *asterisk* indicates $p<0.05$ with respect to the control, *$p<0.05$, **$p<0.01$, ***$p<0.001$.

CHAPTER V

DISCUSSION

The overall aim of the project was to test the anticancer potential of novel cubosomal nanoparticles encapsulting TQ, an anticancer compound extracted from *Nigella sativa*, and compare their activity with free TQ in human breast cancer cell lines *in vitro* and *in vivo*. The cell lines we used included the nontumorigenic MCF-10A breast cells, the aggressive MDA-MB-231 and the MCF-7 breast cancer cell lines. We found that free TQ, blank cubosomes, and TQ-loaded cubosomes, were non-toxic to nontumorigenic MCF-10A breast cells at doses up to 30 µM. Interestingly, the TQ-loaded cubosomes were more cytotoxic than free TQ against human breast cancer MCF-7 and MDA-MB-231 cell lines. This suggested that these cubosomes exert higher anticancer activity than free TQ against breast cancer cells, and thus are a better delivery system for TQ. Microscopic imaging showed that the formulations were taken up by the cells and were localized in the cytoplasm of both cell lines. The cubosomal nanoparticles co-localized with the endocytosis markers clathrin and caveolin, suggesting that endocytosis is the mechanism of cellular trafficking of these nanoparticles. Unexpectedly, the TQ-loaded cubosomes were ineffective *in vivo* as they did not inhibit mouse tumor volume when injected either intraperitoneally or subcutaneously into mice harboring MDA-MB-231 xenografts, suggesting the need to examine other modes of administration into mice.

There are limited studies on the anticancer efficacy of TQ-loaded cubosomal nanoparticles and this is the first comprehensive study documenting their activity and uptake mechanisms. Although studies are limited on TQ-loaded cubosomes, others have

shown that free TQ is cytotoxic to human breast cancer cells (Schneider-Stock, Fakhoury et al. 2014). We have previously prepared a polymeric TQ formulation ($PS_{1600}PEO_{1800}$ amphiphilic diblock polymer) that exhibited suitable physicochemical characteristics (size, encapsulation efficiency, loading capacity and stability) to be considered as a good drug delivery system. The formulation showed an enhanced anticancer activity, in comparison to free TQ, in MCF-7 and MDA-MB-231 breast cancer cell lines and was non-toxic to normal MCF-10A breast cell line, *in vitro* (Fakhoury, Saad et al. 2016). In our system, the obtained IC_{50} values by MTT assay of TQ-loaded cubosomes were 2-3.5 fold lower than that of free TQ in MCF-7 and MDA-MB-231 cell lines, respectively. The obtained IC_{50} value of TQ-loaded cubosomes by trypan blue exclusion test was 1.6 fold lower than that of free TQ in MDA-MB-231 cell line. This enhanced anticancer activity of TQ upon its encapsulation in cubosomes indicates that the nanoparticles improved the delivery of TQ into the cells and as such the same anticancer activity of TQ could be obtained at reduced concentrations. This is most likely due to the fact that more TQ molecules are being delivered to the target site when present in cubosomes.

As mentioned before, viability assays to test the anticancer activities of the various formulations included both MTT and trypan blue exclusion test. The IC_{50} values of the formulations differed between these two assays, particulary for MCF-7 cell line. This could be due to fact that different concentration ranges were used in these assays; the concentrations ranged from 1 to 100 µM in MTT and from 1 to 30 µM in trypan blue. Another reason is that MTT assay measures the metabolically active cells as live cells and those that are arrested in the cell cycle as dead cells; however, in the trypan blue exclusion test only dead cells are stained blue and thus counted. Besides, the

difference in the effect of the blank cubosomes on MDA-MB-231 and MCF-7 cell lines may be due to the difference in their energy metabolic profile. Oleate, the main precursor of cubosomes, acts as a growth factor enhancing the development of MDA-MB-231 cell line by activating the PI3K/AKT/mTOR pathway which, in turn, activates aerobic glycolysis for ATP synthesis. And MDA-MB-231 cell line has a higher expression levels of growth factor receptors and thus higher dependency on glycolysis, in comparison to MCF-7 cell line (Hardy, Langelier et al. 2000, Li, Zhou et al. 2014, Makinoshima, Takita et al. 2015, Manupati, Dhoke et al. 2017, Reda, Refaat et al. 2019).

To understand the mechanism of cell death by TQ-loaded cubosomes, we used several approaches which included DAPI staining of nuclei coupled with confocal microscopy to detect the extent of apoptosis in cells and we measured active caspase-3 by immunoflourescence. Previous studies showed that TQ induced apoptosis and cell cycle arrest in the triple-negative breast cancer (TNBC) with mutant p53, including MDA-MB-231 cell line (Barkat, Harshita et al. 2018). Treatment of MDA-MB-231 cells with 2.5 µM and 5 µM TQ, for 24, 48 and 72 hours, arrested the cells at G1 phase and induced caspase-dependent and independent apoptosis through mitochondrial membrane permeabilization (Sutton, Greenshields et al. 2014). Our results showed that both TQ and TQ-loaded cubosomes induced apoptosis in MDA-MB-231 human breast cancer cells. DAPI staining showed an increase in the apoptotic bodies in the cells treated with either the free or encapsulated form of TQ. In addition, free TQ and TQ-loaded cubosomes significantly increased the cleavage of caspase-3, while blank cubosomes had no significant effect. Caspase-3 is a cysteine protease that is the primary excutioner of the intrinsic apoptotic pathway through mitochondrial permeabilization

and dysfunction (Bressenot, Marchal et al. 2009). Active caspase-3 is the cleaved form of the protease that degrades several target proteins leading to DNA fragmentation. Unlike the viability results, where we obtained a greater activity of TQ-loaded cubosomes, the caspase 3 cleavage results showed that free TQ caused greater caspase 3 cleavage (apoptosis) than TQ-loaded cubosomes. This discrepancy may be due to the differences in the mechanistic effects of TQ *vs* TQ-loaded cubosomes against breast cancer cells. TQ-loaded cubsomes could be inducing cell cycle arrest in addition to apoptosis, while TQ could be causing only apoptotic cell death, a hypothesis that should be tested and confirmed in future experiments.

Our observation that cubosomal nanoparticles were internalized by the breast cancer cells and were localized in the cytoplasm suggests that the formulations reached the cellular target which further explains their enhanced anticancer activity. The uptake of the cubosomal nanoparticles into the cells is indeed important for their drug delivery and treatment efficacy. More importantly, the encapsulation of TQ into cubosomal nanoparticles enabled us to visualize the formulations inside the cells by incorporating a fluorescent dye Nile Red into the nanoparticles. This provides an advantage over the free form of the drug as information about the tumor status and monitoring of the treatment regimens and tumor response to therapy could be obtained (Kievit and Zhang 2011), and as such this increases the possibility of TQ's translation to the clinic.

Interestingly, *in vitro* uptake images showed a significant difference in the distribution of the formulations whereby blank nanoparticles were evenly distributed while the TQ encapsulated nanoparticles showed a punctate distribution. Several factors could affect the uptake, trafficking and distribution of the nanoparticles in the cells. These could include the nanoparticle physicochemical characteristics, biological and

experimental factors, including their sizes, charge, surface chemistry, temperature and ionic strength (Hoshyar, Gray et al. 2016, Behzadi, Serpooshan et al. 2017). Minor changes in the size, solubility and composition (hydrophilicity and hydrophobicity) of the nanoparticles could play a major role in their uptake (De Jong and Borm 2008, Behzadi, Serpooshan et al. 2017). Add to this, TQ is a highly hydrophobic compound and its encapsulation could have caused a change in the composition of the cubosomes and minor changes in their sizes especially when considering that the nanoparticles first interact with the surrounding microenvironment. The microenvironmental properties, including the secreted factors by cells and pH levels could have affected the characteristics of the nanoparticles and their interaction with the cells and subsequent uptake and trafficking by these cells (Behzadi, Serpooshan et al. 2017). This could explain the difference in the distribution pattern of the blank cubosomes *versus* the TQ-loaded cubosomes.

Endocytosis appeared to be the mechanism by which TQ-loaded cubosomes were uptaken by the cells since the formulations colocalized with the antibodies targeting caveolae, clathrin coated pits, early endosomes and lysosomes. Mechanistic studies on the uptake of our previously prepared polymeric TQ formulation showed that the NPs were taken up into the cells by clathrin and caveolin-mediated endocytosis (Fakhoury, Saad et al. 2016). The route and mechanism of entry of the nanoparticles determine their fate inside the cells. Particles taken up by endocytosis are first carried by early endosomes that eventually mature into late endosomes. Late endosomes then fuse with lysosomes forming the endo-lysosomal vesicles that contain hydrolytic enzymes (Foroozandeh and Aziz 2018). Most often, particles taken up by clathrin mediated endocytosis end up in the endo-lysosomal pathway leading to the degradation

of the cargo (Behzadi, Serpooshan et al. 2017, Foroozandeh and Aziz 2018). However, particles taken up by caveosomes may escape lysosomal degradation and be released into the cytoplasm which leads to enhanced drug delivery and therapeutic potential (Behzadi, Serpooshan et al. 2017, Foroozandeh and Aziz 2018). This could be another reason for the enhanced anticancer activity of the TQ-loaded cubsosomes in comparsion to free TQ.

After finding that the TQ-loaded cubosomes had enhanced anticancer effects in comparison to free TQ *in vitro*, these formulations were tested in the MDA-MB-231 xenograft model since documenting *in vivo* efficacy is essential for clinical translation. Several factors could affect the activity of the drugs *in vivo* and thus the enhanced anticancer efficacy of TQ-loaded cubosomes observed *in vitro* may not correlate with the *in vivo* effects. The polymeric TQ-NPs prepared by our lab previously contained the vehicle tetrahydrofuran which was toxic to mice and which could not be evaporated without causing precipitation of the TQ nanoparticles (Fakhoury. 2016). The presence of this toxic vehicle halted its testing in mice as it caused their death when injected intraperitoneally. A literature search showed that the best formulation for injection into animals is based on lipid nanocarriers (cubosomes). Thus, we prepared a safer TQ-NP by encapsulating TQ in cusosomal nanoparticles and tested its efficacy in mice.

Based on our promising *in vitro* findings, we hypothesized that the TQ cubosomal formulation would have enhanced anticancer effects when tested in an animal model of breast cancer. So we treated mice with either free TQ or TQ-loaded cubosomes. However, our *in vivo* findings were not consistent with the *in vitro* activity of the compounds. Instead of observing a decrease in tumor volume, the volume of tumors increased in mice treated intraperitoneally with TQ-loaded cubsomes for 19

days. One reason could be due to the presence of monoolein in the composition of the NPs. This is in accordance with previous literature that has shown that oleate enhances the growth of MDA-MB-231 cell line. A study by Hardy *et al*. showed that oleate acts as a growth factor enhancing the proliferation and survival of MDA-MB-231 cells, at very low concentrations by activating phosphatidylinositol 3-kinase (PI3K) (Hardy, Langelier et al. 2000). Another study by Shuai Li *et al*. showed that highly aggressive carcinoma cells, among which was the MDA-MB-231 cell line, maintained malignancy by AMPK activation when exposed to oleate (Li, Zhou et al. 2014). In turn, AMPK will switch on the ATP-generating metabolic pathways, including fatty acid oxidation, which promote cell proliferation and migration of the aggressive breast cancer cell line (Li, Zhou et al. 2014). In time, the nanoparticle should not have any effect on the tumor and serves as a cargo only, these findings may explain the increase in tumor volume seen in the first *in vivo* experiment.

In the second *in vivo* experiment, tumor volume did not change in mice treated subcutaneously with TQ-loaded cubsomes for 19 days. However, previous studies reported a decrease in tumor volume in mice treated with TQ subcutaneously. Researchers previously showed a decrease in tumor volume and tumor angiogenesis and an inhibition of cell proliferation, in prostate and lung cancer xenograft models in mice, after subcutaneous injection of TQ (Yi, Cho et al. 2008, Jafri, Glass et al. 2010). In our mice experiment, the subcutaneous injection of TQ did not have any effect on the tumor volume. This discrepancy may be due to the site of injection, where subcutaneous injection may be performed in the flank, neck or the abdomenal region. We performed the injections in the loose skin over the neck; however, the site of injection is not mentioned in the previously stated papers. In summary, the tested routes of

administration of TQ-NP did not seem to allow the TQ-loaded cubosomal nanoparticles to reach the targeted tissue which explains the observed lack of efficacy. Future studies should focus on identifying better routes of administering TQ-loaded cubosomes in mice.

Next, we wanted to assess the effects of cubosomal nanoparticles on the proliferation status of the liver, kidney and tumor tissues by quantifying PCNA expression levels. PCNA is a nuclear protein whose expression level gives an indication about cellular proliferation and cell cycle phase. PCNA plays a role in DNA replication, DNA repair and chromatin assembly. It is highly expressed in actively proliferating cells, specifically in S and G2 phases, and very low in quiescent cells (Jurikova, Danihel et al. 2016). In the first *in vivo* experiment, mice treated with blank cubosomes had the largest tumor volumes followed by those treated with TQ-loaded cubosomes then by the control group, while PCNA expression levels were the highest in the tumor tissues of the control group indicating the highest cell proliferation status. Therefore, PCNA expression levels were not in accordance with the tumor volumes. This discrepancy may be explained by the side effects seen in mice treated with blank cubosomes and TQ-loaded cubosomes, including fluid retention. This increase in tumor volume may be due to the accumulation of fluid in the tumor tissues as well, as it was seen at the day of dissection (day 22). H&E images showed that tumor tissues from mice treated with TQ-loaded cubosomes had the lowest number of nuclei (Figure 22). Therefore, the observations of the H&E stains were in accordance with the PCNA expression levels. PCNA expression could not be measured in the tumor tissues of the mice group treated with TQ since the tumor almost disappeared after the 19^{th} day of treatment. In the second *in vivo* experiment, PCNA expression levels were in accordance with the tumor

volumes and the H&E stains. There was a non-significant change in tumor volumes among all mice groups, accompanied by an approximately similar nuclei count and a non-significant change in PCNA expression levels in the tumor tissues, indicating similar cell proliferation status in all groups and similar tumor volumes.

To investigate whether the drug was delivered to the target tissues, we visualized the uptake of the nanoparticles coupled to Nile Red. Cellular uptake images of both *in vivo* experiments did not show any nanoparticles being taken up into the cells except for the tumor tissue from mice treated with blank cubosomes subcutaneously (Figure 23 and 30). This finding indicates that the blank cubosomes are being delivered to the target tissues and taken up by the cells. Among the limitations of TQ are its reduced solubility and bioavailability due to its rapid clearance and slow absorption in the body; more than 99% of TQ are bound to plasma proteins (Jain 2000, El-Najjar, Ketola et al. 2011, Alkharfy, Ahmad et al. 2015, Asaduzzaman Khan, Tania et al. 2017). These limitations were overcome by this formulation; therefore, showing that cubosomal nanoparticles are good drug-delivery systems. However, the negative signal in the remaining tissues may be due to several reasons. Several factors control the circulation, biodistribution and uptake of the nanoparticles into the organs and cells. The size, surface charge and shape of the nanoparticles, as well as their interaction with the bioenvironment affect their biochemical properties and thus affecting their metabolism and trafficking in the organism (Wang, He et al. 2013). Cellular uptake and trafficking of nanoparticles are still a challenge. We performed mice dissection at day 22, which is 3 days after the last treatment day. One possibility is that the nanoparticles got metabolized during this delayed time from treatment. These factors may explain the negative signal in the uptake images.

In summary, TQ's anticancer activity was enhanced upon its encapsulation in cubosomal nanoparticles, *in vitro*. However, further studies are required to optimize the route of administration in animal models. Some of TQ's limitations, among which its low bioavailability and binding to plasma proteins, were overcome by its encapsulation in the nanoparticles. Besides, the visualization and tracking of the formulations became possible, in comparison to free TQ. This project forms a platform for the discovery of a novel drug and its possible translation to the clinic. Future studies necessitate the investigation of the involved signalling pathways and the key targeted molecules that are responsible for the enhanced activity of the cubosomal nanoparticles against breast cancer cell lines.

CHAPTER VI

BIBLIOGRAPHY

Akram, M. and S. A. Siddiqui (2012). "Breast cancer management: past, present and evolving." Indian J Cancer **49**(3): 277-282.

Alhosin, M., A. Abusnina, M. Achour, T. Sharif, C. Muller, J. Peluso, T. Chataigneau, C. Lugnier, V. B. Schini-Kerth, C. Bronner and G. Fuhrmann (2010). "Induction of apoptosis by thymoquinone in lymphoblastic leukemia Jurkat cells is mediated by a p73-dependent pathway which targets the epigenetic integrator UHRF1." Biochem Pharmacol **79**(9): 1251-1260.

Alkharfy, K. M., A. Ahmad, R. M. Khan and W. M. Al-Shagha (2015). "Pharmacokinetic plasma behaviors of intravenous and oral bioavailability of thymoquinone in a rabbit model." Eur J Drug Metab Pharmacokinet **40**(3): 319-323.

Allred, D. C. (2010). "Ductal carcinoma in situ: terminology, classification, and natural history." J Natl Cancer Inst Monogr **2010**(41): 134-138.

Asaduzzaman Khan, M., M. Tania, S. Fu and J. Fu (2017). "Thymoquinone, as an anticancer molecule: from basic research to clinical investigation." Oncotarget **8**(31): 51907-51919.

Attoub, S., O. Sperandio, H. Raza, K. Arafat, S. Al-Salam, M. A. Al Sultan, M. Al Safi, T. Takahashi and A. Adem (2013). "Thymoquinone as an anticancer agent: evidence from inhibition of cancer cells viability and invasion in vitro and tumor growth in vivo." Fundam Clin Pharmacol **27**(5): 557-569.

Azad, N., C. A. Zahnow, C. M. Rudin and S. B. Baylin (2013). "The future of epigenetic therapy in solid tumours--lessons from the past." Nat Rev Clin Oncol **10**(5): 256-266.

Ballout, F., Z. Habli, O. N. Rahal, M. Fatfat and H. Gali-Muhtasib (2018). "Thymoquinone-based nanotechnology for cancer therapy: promises and challenges." Drug Discov Today **23**(5): 1089-1098.

Barkat, M. A., Harshita, J. Ahmad, M. A. Khan, S. Beg and F. J. Ahmad (2018). "Insights into the Targeting Potential of Thymoquinone for Therapeutic Intervention Against Triple-negative Breast Cancer." Curr Drug Targets **19**(1): 70-80.

Barreto, J. A., W. O'Malley, M. Kubeil, B. Graham, H. Stephan and L. Spiccia (2011). "Nanomaterials: applications in cancer imaging and therapy." Adv Mater **23**(12): H18-40.

Bazak, R., M. Houri, S. El Achy, S. Kamel and T. Refaat (2015). "Cancer active targeting by nanoparticles: a comprehensive review of literature." J Cancer Res Clin Oncol **141**(5): 769-784.

Behzadi, S., V. Serpooshan, W. Tao, M. A. Hamaly, M. Y. Alkawareek, E. C. Dreaden, D. Brown, A. M. Alkilany, O. C. Farokhzad and M. Mahmoudi (2017). "Cellular uptake of nanoparticles: journey inside the cell." Chem Soc Rev **46**(14): 4218-4244.

Bertos, N. R. and M. Park (2011). "Breast cancer - one term, many entities?" J Clin Invest **121**(10): 3789-3796.

Bhattacharya, S., M. Ahir, P. Patra, S. Mukherjee, S. Ghosh, M. Mazumdar, S. Chattopadhyay, T. Das, D. Chattopadhyay and A. Adhikary (2015). "PEGylated-thymoquinone-nanoparticle mediated retardation of breast cancer cell migration by deregulation of cytoskeletal actin polymerization through miR-34a." Biomaterials **51**: 91-107.

Bodai, B. I. and P. Tuso (2015). "Breast cancer survivorship: a comprehensive review of long-term medical issues and lifestyle recommendations." Perm J **19**(2): 48-79.

Bovelli, D., G. Plataniotis, F. Roila and E. G. W. Group (2010). "Cardiotoxicity of chemotherapeutic agents and radiotherapy-related heart disease: ESMO Clinical Practice Guidelines." Ann Oncol **21 Suppl 5**: v277-282.

Bray, F., J. Ferlay, I. Soerjomataram, R. L. Siegel, L. A. Torre and A. Jemal (2018). "Global cancer statistics 2018: GLOBOCAN estimates of incidence and mortality worldwide for 36 cancers in 185 countries." CA Cancer J Clin **68**(6): 394-424.

Bressenot, A., S. Marchal, L. Bezdetnaya, J. Garrier, F. Guillemin and F. Plenat (2009). "Assessment of apoptosis by immunohistochemistry to active caspase-3, active caspase-7, or cleaved PARP in monolayer cells and spheroid and subcutaneous xenografts of human carcinoma." J Histochem Cytochem **57**(4): 289-300.

Comsa, S., A. M. Cimpean and M. Raica (2015). "The Story of MCF-7 Breast Cancer Cell Line: 40 years of Experience in Research." Anticancer Res **35**(6): 3147-3154.

Cronin, K. A., A. J. Lake, S. Scott, R. L. Sherman, A. M. Noone, N. Howlader, S. J. Henley, R. N. Anderson, A. U. Firth, J. Ma, B. A. Kohler and A. Jemal (2018). "Annual Report to the Nation on the Status of Cancer, part I: National cancer statistics." Cancer **124**(13): 2785-2800.

Das, S. and A. Chaudhury (2011). "Recent advances in lipid nanoparticle formulations with solid matrix for oral drug delivery." AAPS PharmSciTech **12**(1): 62-76.

Das, S., K. K. Dey, G. Dey, I. Pal, A. Majumder, S. MaitiChoudhury, S. C. kundu and M. Mandal (2012). "Antineoplastic and apoptotic potential of traditional medicines thymoquinone and diosgenin in squamous cell carcinoma." PLoS One **7**(10): e46641.

Dastjerdi, M. N., E. M. Mehdiabady, F. G. Iranpour and H. Bahramian (2016). "Effect of Thymoquinone on P53 Gene Expression and Consequence Apoptosis in Breast Cancer Cell Line." Int J Prev Med **7**: 66.

De Jong, W. H. and P. J. Borm (2008). "Drug delivery and nanoparticles:applications and hazards." Int J Nanomedicine **3**(2): 133-149.

El-Najjar, N., R. A. Ketola, T. Nissila, T. Mauriala, M. Antopolsky, J. Janis, H. Gali-Muhtasib, A. Urtti and H. Vuorela (2011). "Impact of protein binding on the analytical detectability and anticancer activity of thymoquinone." J Chem Biol **4**(3): 97-107.

Fakhoury, I., W. Saad, K. Bouhadir, P. Nygren, R. Schneider-Stock and H. Gali-Muhtasib (2016). "Uptake, delivery, and anticancer activity of thymoquinone nanoparticles in breast cancer cells." Journal of Nanoparticle Research **18**(7): 210.

Foroozandeh, P. and A. A. Aziz (2018). "Insight into Cellular Uptake and Intracellular Trafficking of Nanoparticles." Nanoscale Res Lett **13**(1): 339.

Gali-Muhtasib, H., M. Diab-Assaf, C. Boltze, J. Al-Hmaira, R. Hartig, A. Roessner and R. Schneider-Stock (2004). "Thymoquinone extracted from black seed triggers apoptotic cell death in human colorectal cancer cells via a p53-dependent mechanism." Int J Oncol **25**(4): 857-866.

Gali-Muhtasib, H. U., W. G. Abou Kheir, L. A. Kheir, N. Darwiche and P. A. Crooks (2004). "Molecular pathway for thymoquinone-induced cell-cycle arrest and apoptosis in neoplastic keratinocytes." Anticancer Drugs **15**(4): 389-399.

Glozak, M. A. and E. Seto (2007). "Histone deacetylases and cancer." Oncogene **26**(37): 5420-5432.

Hamurcu, Z., A. Ashour, N. Kahraman and B. Ozpolat (2016). "FOXM1 regulates expression of eukaryotic elongation factor 2 kinase and promotes proliferation, invasion and tumorgenesis of human triple negative breast cancer cells." Oncotarget **7**(13): 16619-16635.

Hardy, S., Y. Langelier and M. Prentki (2000). "Oleate activates phosphatidylinositol 3-kinase and promotes proliferation and reduces apoptosis of MDA-MB-231 breast cancer cells, whereas palmitate has opposite effects." Cancer Res **60**(22): 6353-6358.

Hoshyar, N., S. Gray, H. Han and G. Bao (2016). "The effect of nanoparticle size on in vivo pharmacokinetics and cellular interaction." Nanomedicine (Lond) **11**(6): 673-692.

Jafri, S. H., J. Glass, R. Shi, S. Zhang, M. Prince and H. Kleiner-Hancock (2010). "Thymoquinone and cisplatin as a therapeutic combination in lung cancer: In vitro and in vivo." J Exp Clin Cancer Res **29**: 87.

Jain, R. A. (2000). "The manufacturing techniques of various drug loaded biodegradable poly(lactide-co-glycolide) (PLGA) devices." Biomaterials **21**(23): 2475-2490.

Jurikova, M., L. Danihel, S. Polak and I. Varga (2016). "Ki67, PCNA, and MCM proteins: Markers of proliferation in the diagnosis of breast cancer." Acta Histochem **118**(5): 544-552.

Kabil, N., R. Bayraktar, N. Kahraman, H. A. Mokhlis, G. A. Calin, G. Lopez-Berestein and B. Ozpolat (2018). "Thymoquinone inhibits cell proliferation, migration, and invasion by regulating the elongation factor 2 kinase (eEF-2K) signaling axis in triple-negative breast cancer." Breast Cancer Res Treat **171**(3): 593-605.

Khan, M. A., M. Tania, C. Wei, Z. Mei, S. Fu, J. Cheng, J. Xu and J. Fu (2015). "Thymoquinone inhibits cancer metastasis by downregulating TWIST1 expression to reduce epithelial to mesenchymal transition." Oncotarget **6**(23): 19580-19591.

Kievit, F. M. and M. Zhang (2011). "Cancer nanotheranostics: improving imaging and therapy by targeted delivery across biological barriers." Adv Mater **23**(36): H217-247.

Kluzek, M., A. I. I. Tyler, S. Wang, R. Chen, C. M. Marques, F. Thalmann, J. M. Seddon and M. Schmutz (2017). "Influence of a pH-sensitive polymer on the structure of monoolein cubosomes." Soft Matter **13**(41): 7571-7577.

Kumari, A., S. K. Yadav and S. C. Yadav (2010). "Biodegradable polymeric nanoparticles based drug delivery systems." Colloids Surf B Biointerfaces **75**(1): 1-18.

Lee, A. V., S. Oesterreich and N. E. Davidson (2015). "MCF-7 cells--changing the course of breast cancer research and care for 45 years." J Natl Cancer Inst **107**(7).

Li, F., P. Rajendran and G. Sethi (2010). "Thymoquinone inhibits proliferation, induces apoptosis and chemosensitizes human multiple myeloma cells through suppression of signal transducer and activator of transcription 3 activation pathway." Br J Pharmacol **161**(3): 541-554.

Li, S., T. Zhou, C. Li, Z. Dai, D. Che, Y. Yao, L. Li, J. Ma, X. Yang and G. Gao (2014). "High metastaticgastric and breast cancer cells consume oleic acid in an AMPK dependent manner." PLoS One **9**(5): e97330.

Liu, K., P. A. Newbury, B. S. Glicksberg, W. Z. D. Zeng, S. Paithankar, E. R. Andrechek and B. Chen (2019). "Evaluating cell lines as models for metastatic breast cancer through integrative analysis of genomic data." Nat Commun **10**(1): 2138.

Makinoshima, H., M. Takita, K. Saruwatari, S. Umemura, Y. Obata, G. Ishii, S. Matsumoto, E. Sugiyama, A. Ochiai, R. Abe, K. Goto, H. Esumi and K. Tsuchihara (2015). "Signaling through the Phosphatidylinositol 3-Kinase (PI3K)/Mammalian Target of Rapamycin (mTOR) Axis Is Responsible for Aerobic Glycolysis mediated by Glucose Transporter in Epidermal Growth Factor Receptor (EGFR)-mutated Lung Adenocarcinoma." J Biol Chem **290**(28): 17495-17504.

Manupati, K., N. R. Dhoke, T. Debnath, R. Yeeravalli, K. Guguloth, S. Saeidpour, U. C. De, S. Debnath and A. Das (2017). "Inhibiting epidermal growth factor receptor signalling potentiates mesenchymal-epithelial transition of breast cancer stem cells and their responsiveness to anticancer drugs." FEBS J **284**(12): 1830-1854.

Matsen, C. B. and L. A. Neumayer (2013). "Breast cancer: a review for the general surgeon." JAMA Surg **148**(10): 971-979.

Mohyeldin, S. M., M. M. Mehanna and N. A. Elgindy (2016). "Superiority of liquid crystalline cubic nanocarriers as hormonal transdermal vehicle: comparative human skin permeation-supported evidence." Expert Opin Drug Deliv **13**(8): 1049-1064.

Murgia, S., S. Bonacchi, A. M. Falchi, S. Lampis, V. Lippolis, V. Meli, M. Monduzzi, L. Prodi, J. Schmidt, Y. Talmon and C. Caltagirone (2013). "Drug-loaded fluorescent cubosomes: versatile nanoparticles for potential theranostic applications." Langmuir **29**(22): 6673-6679.

Nazaruk, E., A. Majkowska-Pilip and R. Bilewicz (2017). "Lipidic Cubic-Phase Nanoparticles—Cubosomes for Efficient Drug Delivery to Cancer Cells." ChemPlusChem **82**(4): 570-575.

Ng, W. K., L. Saiful Yazan, L. H. Yap, W. A. Wan Nor Hafiza, C. W. How and R. Abdullah (2015). "Thymoquinone-loaded nanostructured lipid carrier exhibited cytotoxicity towards breast cancer cell lines (MDA-MB-231 and MCF-7) and cervical cancer cell lines (HeLa and SiHa)." Biomed Res Int **2015**: 263131.

Nounou, M. I., F. ElAmrawy, N. Ahmed, K. Abdelraouf, S. Goda and H. Syed-Sha-Qhattal (2015). "Breast Cancer: Conventional Diagnosis and Treatment Modalities and Recent Patents and Technologies." Breast Cancer (Auckl) **9**(Suppl 2): 17-34.

Odeh, F., S. I. Ismail, R. Abu-Dahab, I. S. Mahmoud and A. Al Bawab (2012). "Thymoquinone in liposomes: a study of loading efficiency and biological activity towards breast cancer." Drug Deliv **19**(8): 371-377.

Parbin, S., A. Shilpi, S. Kar, N. Pradhan, D. Sengupta, M. Deb, S. K. Rath and S. K. Patra (2016). "Insights into the molecular interactions of thymoquinone with histone deacetylase: evaluation of the therapeutic intervention potential against breast cancer." Mol Biosyst **12**(1): 48-58.

Pathan, S. A., G. K. Jain, S. M. Zaidi, S. Akhter, D. Vohora, P. Chander, P. L. Kole, F. J. Ahmad and R. K. Khar (2011). "Stability-indicating ultra-performance liquid chromatography method for the estimation of thymoquinone and its application in biopharmaceutical studies." Biomed Chromatogr **25**(5): 613-620.

Petschauer, J. S., A. J. Madden, W. P. Kirschbrown, G. Song and W. C. Zamboni (2015). "The effects of nanoparticle drug loading on the pharmacokinetics of anticancer agents." Nanomedicine (Lond) **10**(3): 447-463.

Qu, Y., B. Han, Y. Yu, W. Yao, S. Bose, B. Y. Karlan, A. E. Giuliano and X. Cui (2015). "Evaluation of MCF10A as a Reliable Model for Normal Human Mammary Epithelial Cells." PLoS One **10**(7): e0131285.

Rajput, S., B. N. Kumar, K. K. Dey, I. Pal, A. Parekh and M. Mandal (2013). "Molecular targeting of Akt by thymoquinone promotes G(1) arrest through translation inhibition of cyclin D1 and induces apoptosis in breast cancer cells." Life Sci **93**(21): 783-790.

Reda, A., A. Refaat, A. A. Abd-Rabou, A. M. Mahmoud, M. Adel, S. Sabet and S. S. Ali (2019). "Role of mitochondria in rescuing glycolytically inhibited subpopulation of triple negative but not hormone-responsive breast cancer cells." Scientific Reports **9**(1): 13748.

Samarghandian, S., M. Azimi-Nezhad and T. Farkhondeh (2018). "Thymoquinone-induced antitumor and apoptosis in human lung adenocarcinoma cells." J Cell Physiol.

Schneider-Stock, R., I. H. Fakhoury, A. M. Zaki, C. O. El-Baba and H. U. Gali-Muhtasib (2014). "Thymoquinone: fifty years of success in the battle against cancer models." Drug Discov Today **19**(1): 18-30.

Senapati, S., A. K. Mahanta, S. Kumar and P. Maiti (2018). "Controlled drug delivery vehicles for cancer treatment and their performance." Signal Transduct Target Ther **3**: 7.

Shanmugam, M. K., K. S. Ahn, A. Hsu, C. C. Woo, Y. Yuan, K. H. B. Tan, A. Chinnathambi, T. A. Alahmadi, S. A. Alharbi, A. P. F. Koh, F. Arfuso, R. Y. Huang, L. H. K. Lim, G. Sethi and A. P. Kumar (2018). "Thymoquinone Inhibits Bone Metastasis of Breast Cancer Cells Through Abrogation of the CXCR4 Signaling Axis." Front Pharmacol **9**: 1294.

Shanmugam, M. K., A. Hsu, K. M. Hui, B. K. H. Tan and G. Sethi (2016). "Abstract 4123: Thymoquinone inhibits bone metastasis in a breast cancer mouse model by modulating CXCR4/CXCL12 signaling axis." Cancer Research **76**(14 Supplement): 4123-4123.

Shultz, L. D., N. Goodwin, F. Ishikawa, V. Hosur, B. L. Lyons and D. L. Greiner (2014). "Human cancer growth and therapy in immunodeficient mouse models." Cold Spring Harb Protoc **2014**(7): 694-708.

Siegel, R. L., K. D. Miller and A. Jemal (2019). "Cancer statistics, 2019." CA Cancer J Clin **69**(1): 7-34.

Siemann, D. W. (2011). "The unique characteristics of tumor vasculature and preclinical evidence for its selective disruption by Tumor-Vascular Disrupting Agents." Cancer Treat Rev **37**(1): 63-74.

Souza, S. (2014). "A Review of In Vitro Drug Release Test Methods for Nano-Sized Dosage Forms." Advances in Pharmaceutics **2014**: 12.

Subburayan, K., F. Thayyullathil, S. Pallichankandy, A. Rahman and S. Galadari (2018). "Par-4-dependent p53 up-regulation plays a critical role in thymoquinone-induced cellular senescence in human malignant glioma cells." Cancer Lett **426**: 80-97.

Sun, Y. S., Z. Zhao, Z. N. Yang, F. Xu, H. J. Lu, Z. Y. Zhu, W. Shi, J. Jiang, P. P. Yao and H. P. Zhu (2017). "Risk Factors and Preventions of Breast Cancer." Int J Biol Sci **13**(11): 1387-1397.

Sutton, K. M., A. L. Greenshields and D. W. Hoskin (2014). "Thymoquinone, a bioactive component of black caraway seeds, causes G1 phase cell cycle arrest and apoptosis in triple-negative breast cancer cells with mutant p53." Nutr Cancer **66**(3): 408-418.

Viallard, C. and B. Larrivee (2017). "Tumor angiogenesis and vascular normalization: alternative therapeutic targets." Angiogenesis **20**(4): 409-426.

Wang, A. Z., R. Langer and O. C. Farokhzad (2012). "Nanoparticle delivery of cancer drugs." Annu Rev Med **63**: 185-198.

Wang, B., X. He, Z. Zhang, Y. Zhao and W. Feng (2013). "Metabolism of nanomaterials in vivo: blood circulation and organ clearance." Acc Chem Res **46**(3): 761-769.

Weigelt, B., F. C. Geyer and J. S. Reis-Filho (2010). "Histological types of breast cancer: how special are they?" Mol Oncol **4**(3): 192-208.

Woo, C. C., A. Hsu, A. P. Kumar, G. Sethi and K. H. Tan (2013). "Thymoquinone inhibits tumor growth and induces apoptosis in a breast cancer xenograft mouse model: the role of p38 MAPK and ROS." PLoS One **8**(10): e75356.

Yang, J., X. R. Kuang, P. T. Lv and X. X. Yan (2015). "Thymoquinone inhibits proliferation and invasion of human nonsmall-cell lung cancer cells via ERK pathway." Tumour Biol **36**(1): 259-269.

Yi, T., S. G. Cho, Z. Yi, X. Pang, M. Rodriguez, Y. Wang, G. Sethi, B. B. Aggarwal and M. Liu (2008). "Thymoquinone inhibits tumor angiogenesis and tumor growth through suppressing AKT and extracellular signal-regulated kinase signaling pathways." Mol Cancer Ther **7**(7): 1789-1796.

Zhang, L., Y. Bai and Y. Yang (2016). "Thymoquinone chemosensitizes colon cancer cells through inhibition of NF-kappaB." Oncol Lett **12**(4): 2840-2845.